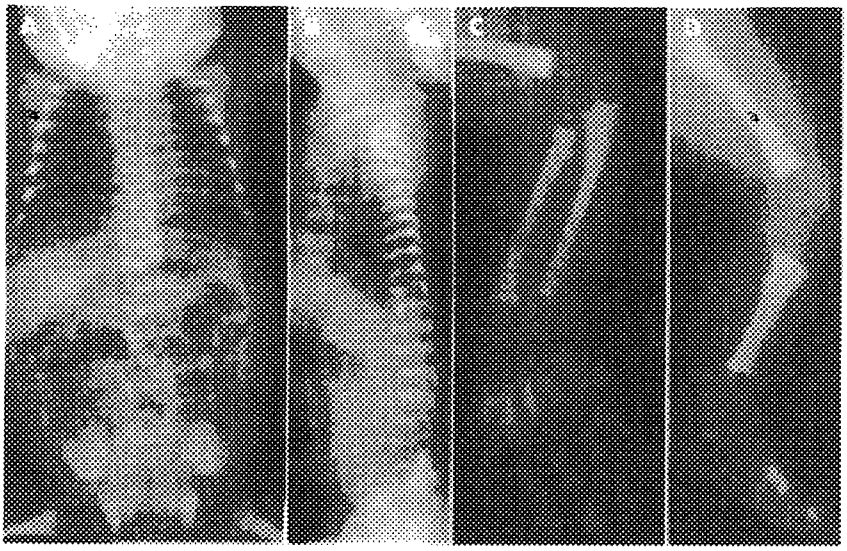

Figure 1 Radiographs of patient 1 at age 1 day: chest and abdomen (A), lateral spine (B), arm (C) and leg (D). Note the narrow thorax, short ribs with cupped anterior ends, severe dense platyspondyly, lacy iliac crests, delayed ossification of the caudal ilia, and metaphysial cupping and irregularity of the tubular bones. The proximal femoral metaphysis has a faded area with a rounded end, similar to what is seen in spondylometaphysial dysplasia Sedaghatian type.

and metaphysial cupping of the short tubular bones (figs 2 and 3). The radiological findings in childhood were interpreted as an unclassifiable metaphysial dysplasia.

Patient 2

This boy was the product of the first pregnancy of a healthy, non-consanguineous British couple. Fetal ultrasound at 17 weeks gestation was reported to be normal. A macerated stillbirth was delivered at full term. The weight was below the 1st centile for a full-term infant. Physical findings included a narrow thorax and rhizomelic shortening of the limbs. A postmortem radiograph showed thoracic hypoplasia with horizontal short ribs, mild platyspondyly, ragged iliac crests, delayed ossification of the caudal ilia, hypoplastic pubic rami, and ragged, cupped metaphyses of the long bones (fig 4). A review at the European Skeletal Dysplasia Network review panel (www.esdn.org) concluded that the skeletal changes are suggestive of SMD Sedaghatian type. Autopsy showed atrial septal defect, hypoplasia of the gallbladder and distended ileal loops filled with meconium. Histological examination showed periportal hepatic fibrosis, calcifications in dilated renal tubules and pulmonary hypoplasia (lung:body weight ratio = 0.006; <0.012 indicates lethal hypoplasia) (fig 5a). The pancreas appeared unremarkable, although tissue preservation was poor. Chondro-osseous histology showed cystic foci with neighbouring pyknotic chondrocytes in the resting zone. Cartilage columns in the hypertrophic zone were poorly organised, and cartilaginous spicules extended into the metaphysis (fig 5b). Elongation of the hypertrophic zones was modest.

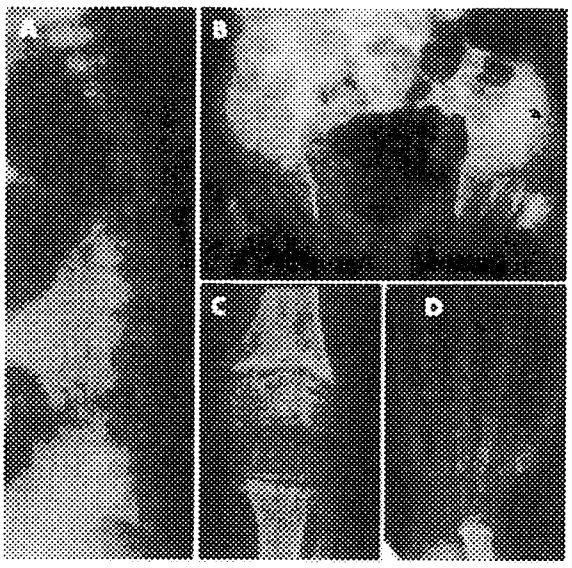

Figure 2 Radiographs of patient 1 at age 5 years: lateral spine (A), pelvis (B), knee (C) and hand (D). Note posteriorly wedged vertebral bodies without platyspondyly, iliac base hypoplasia, metaphysial irregularity with epiphysial plate widening and large epiphyses of the long bones, and metaphysial cupping of the short tubular bones.

Molecular analysis

Peripheral blood from patient 1 and skin from patient 2 were obtained with informed consent from their parents. Genomic DNAs were extracted using standard procedures. *SBDS* mutation analysis was carried out as described previously.[12] Patient 1 was a compound heterozygote for two *SBDS* mutations, 79T→C and 183TA→ CT, and patient 2 carried 183TA→CT and 258+2T→C mutations (fig 6). 79T→C is a novel missense mutation (F27L) that was not found in 70 Japanese control subjects. Codon 27 resides in the N-terminal (FYSH) domain where *SBDS* mutations often occur,[2 4] and it is highly conserved among various species from archaea to mammals. Both 183TA→CT (K62X) and 258+2T→C (C84fsX3) are recurrent mutations that are caused by gene conversion.[2 12] No other sequence variations were found. The parents were unwilling to undergo molecular analysis. We also examined *SBDS* in neonatal SMD: five cases from the International Skeletal

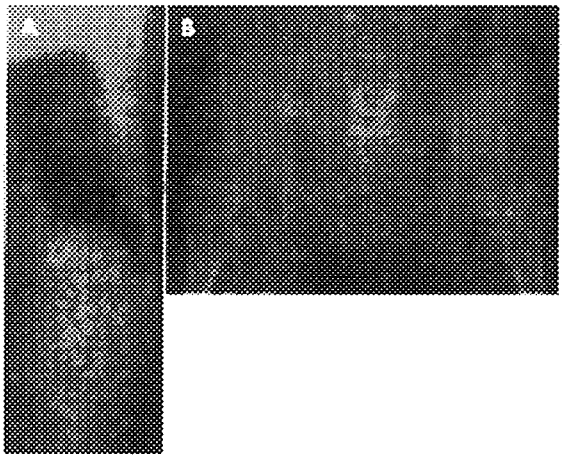

Figure 3 Radiographs of patient 1 at age 11 years: lateral spine (A) and pelvis (B). Note the flared, cupped anterior ends of the ribs, normal height of the vertebral bodies, iliac hypoplasia and continuing metaphysial changes of the proximal femora.

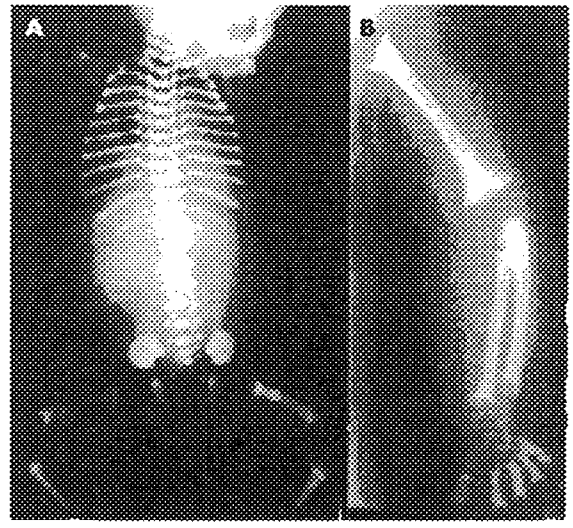

Figure 4 A postmortem radiograph of patient 2: babygram (A) and magnification view of the arm (B). Note the thoracic hypoplasia with horizontal short ribs, mild platyspondyly, ragged iliac crests, delayed ossification of the caudal ilia, hypoplastic pubic rami, and ragged, cupped metaphyses of the long bones.

Dysplasia Registry (http://www.CSMS.edu/3805.html), including a previously reported case with SMD Sedaghatian type[13] and four cases from the European Skeletal Dysplasia Network (http://www.esdn.org/). No *SBDS* mutations were found in these cases.

DISCUSSION

The skeletal phenotype of SDS is classified within the metaphysial dysplasia group.[14] The cardinal skeletal findings include metaphysial irregularities of the long bones, particularly of the proximal femora, and short ribs with flared, cupped anterior ends.[15] Both findings are generally mild. The former rarely manifests in the neonatal period.[16] The latter may occasionally cause respiratory distress in the affected neonates, but they survive the neonatal period.[10 16] The spine is normal in SDS. In classical SDS, the discrete skeletal signs are often sought to confirm a diagnosis that is suspected because of the extraskeletal features, namely, neutropenia or pancreatic insufficiency, and failure to thrive.

The radiological diagnosis of metaphysial dysplasia in childhood and the presence of neutropenia led us to investigate the *SBDS* gene in patient 1, which showed compound heterozygotic *SBDS* mutations in the girl. Her decreased serum isoamylase may have represented sub-clinical exocrine pancreatic insufficiency. However, her skeletal phenotypes were much more severe than what is typically seen in SDS.[17] The skeletal changes in childhood, including severe thoracic hypoplasia, iliac hypoplasia, mega-epiphyses of the long bones and metaphysial cupping of the short tubular bones, were unusual for SDS. Furthermore, she presented with a form of SMD in the neonatal period causing severe respiratory distress. The phenotype was considered a mild form of SMD Sedaghatian type. Observation of the *SBDS* mutations in the girl led to investigation of the *SBDS* gene in other cases with a diagnosis of SMD Sedaghatian type, which discovered one more patient positive for *SBDS* mutations (patient 2). In retrospect, hepatic fibrosis in the boy was accounted for by *SBDS* mutations.

SMD Sedaghatian type is a rare lethal skeletal dysplasia inherited as an autosomal recessive trait.[11 13 18-22] Most affected individuals succumbed in the perinatal period, and the longest survivor died 161 days after birth. The skeletal hallmarks of the disorder include a narrow thorax, moderate platyspondyly, metaphysial cupping and irregularity of the tubular bones, delayed ossification of the caudal ilia and, most distinctively, "lacy iliac crests". These skeletal changes are reflected in the chondro-osseous morphology of the disorder, that is, long hypertrophic zones with hypercellularity and little matrix extending into the metaphyses.[13 18 19] The skeletal changes in the present patients were qualitatively similar to, but milder than, those of previously reported cases with SMD Sedaghatian type from the viewpoint of severity of metaphysial dysplasia, platyspondyly and delayed ossification of the caudal ilia. The somewhat milder skeletal changes seen in our two mutation-positive patients may be correlated with the histological finding of moderate elongation of the hypertrophic zone found in patient 2, as opposed to the significant hypertrophic cell elongation seen in typical SMD Sedaghatian type. Extraskeletal abnormalities have been reported in SMD Sedaghatian type, and include cardiomyopathy and migration anomalies of the brain.[11 13 21] However, neither haematological nor pancreatic abnormalities have been described in the disorder so far.

The present patients harboured one or both of the common *SBDS* mutations—that is, 183–184TA→CT and 258+2T→C. As no homozygote for 183–184TA→CT has been observed, the mutation may create complete loss of function of the SBDS protein with lethality in the homozygotic state—that is, a null mutation due to a stop codon. On the other hand, homozygosity of 258+2T→C and compound heterozygosity of 183–184TA→CT and 258+2T→C are prevalent in patients with SDS.[2 23] While the 258+2T→C mutation predicts aberrant splicing with a premature termination codon, a small amount of the SBDS protein has been observed by immunoblotting with an antibody against the C-terminus of the SBDS protein in a 258+2T→C homozygote.[24] Thus, variable amounts of the functional protein in affected individuals determine variable biological consequences of 258+2T→C. In fact, the clinical phenotypes of compound heterozygotes of 183–184TA→CT and 258+2T→C are quite variable. For example, the height of the patients ranges from −1 SD to −4.5 SD.[17] Thus, the severe phenotypes of patients 1 and 2 are attributable to a non-functional allele (183–184TA→CT) and an allele with a trace amount of expression of the functional protein (258+2T→C).

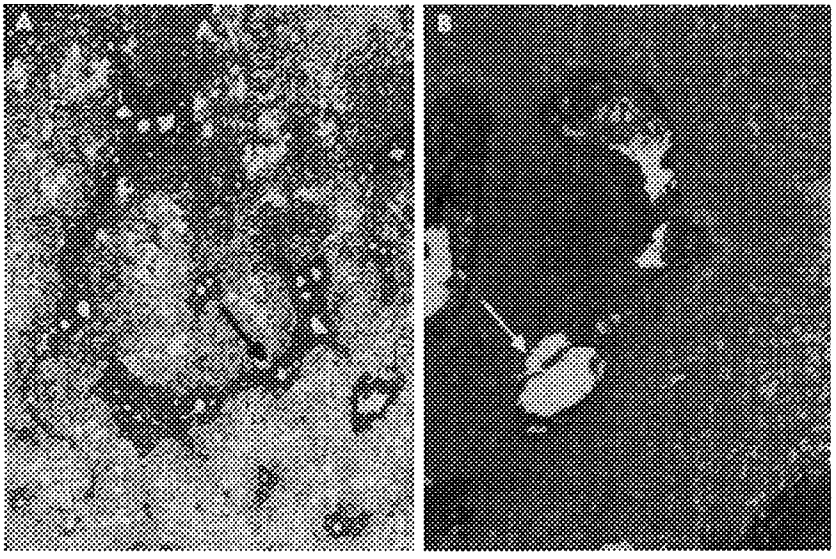

Figure 5 Histological examination of patient 2: liver with reticulin staining (A) and chondro-osseous junction of the femur with haematoxylin and eosin staining (B). Note periportal hepatic fibrosis in the liver (black arrow). The chondro-osseous junction shows foci of cystic lesions in the resting zone (white arrow) and poorly organised cartilage columns of the hypertrophic zone.

We assume that 79T→C found in patient 1 is a disease-causing mutation because it is predicted to cause a missense change of an evolutionally conserved amino acid; the amino acid is located in a mutation-clustered domain of the *SBDS* gene.[2 4] Our assumption is supported by the fact that it is not found in the polymorphism database and in a considerable number of ethnicity-matched controls. However, a possibility that it is a functionally innocent polymorphism cannot be totally excluded at present, because the function of the SBDS protein is currently unknown, and hence no functional assay for the SBDS protein is available. The severe phenotype of the patient suggests that the biological consequence of 79T→C may be deleterious. Further studies are necessary to clarify its functional impact.

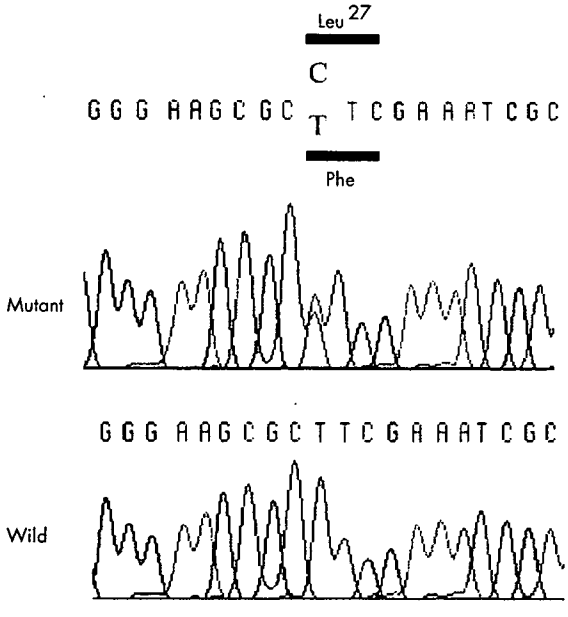

Figure 6 A novel missense mutation (79T→C) in exon 1 of *Shwachman–Bodian–Diamond syndrome* in patient 1.

We also examined the *SBDS* gene in nine other cases with a diagnosis of neonatal SMD, including a case that had been previously reported as a typical SMD Sedaghatian type.[13] However, no SBDS mutations were found in these patients. Implications of our experiences are as follows: *SBDS* mutations give rise to variable phenotypes, including typical SDS and neonatal SMD resembling SMD Sedaghatian type. The latter phenotype may be related to the heterozygosity of 183–184TA→CT, the homozygosity of which is assumed to cause the lethality. Classical SMD Sedaghatian type is a different entity in that no causal gene has been identified. The differences in extraskeletal manifestations may help in distinguishing neonatal SMD due to *SBDS* mutations from classical SMD Sedaghatian type, although these distinctions may be difficult in patients who do not survive the neonatal period.

ACKNOWLEDGEMENTS

We thank Drs Kayoko Takahashi and Yukikatsu Ochiai (Department of Pediatrics, Tokyo Metropolitan Kita Medical Rehabilitation Center for the Handicapped, Tokyo, Japan) for giving us the clinical information of patient 1, and Dr Christine Hall (Department of Radiology, Great Ormond St Children's Hospital, London, UK) as well as the European Skeletal Dysplasia Network review panel for diagnostic review of patient 2. Supported in part by the following grants: Grant-in-Aid from Research on Child Health and Development (Contract Grant No: 17C-1; H18-005); EU grant QLGI-CT2001-02188 (European Union) and Swiss OFES-BBW grant 01.258 (Switzerland; both to the ESDN network); a USPHS NIH Program Project Grant (HD- PO1-HD 22657)(USA) and an NIH GCRC Grant M01-RR00425 from the National Center for Research Resources (USA).

Authors' affiliations
Gen Nishimura, Eiji Nakashima, Hirofumi Ohashi, Shiro Ikegawa, Japanese Skeletal Dysplasia Consortium, Tokyo, Japan

Key points

- We report on two patients with neonatal spondylometaphysial dysplasia (SMD) caused by compound heterozygotic mutations in the *Shwachman–Bodian–Diamond syndrome (SBDS)* gene. This is the second report of the disease caused by mutations in the *SBDS* gene.
- Skeletal features of the patients resembled those of SMD Sedaghatian type, which is basically lethal in the neonatal period. This is the first report of the mutation in a neonatal form of SMD.
- *SBDS* mutations were not found in nine additional cases with neonatal SMD including one typical case with SMD Sedaghantian type. *SBDS* mutations give rise to variable phenotypes, including typical Shwachman–Diamond syndrome and Sedaghatian-like neonatal SMD. Classical SMD Sedaghatian type is a different entity in that no causal gene has been identified.

Gen Nishimura, Department of Radiology, Tokyo Metropolitan Kiyose Children's Hospital, Kiyose, Japan
Eiji Nakashima, Yuichiro Hirose, Yoshinari Miyamoto, Shiro Ikegawa, Laboratory for Bone and Joint Diseases, SNP Research Center, RIKEN, Tokyo, Japan
Trevor Cole, Department of Clinical Genetics, Birmingham Women's Hospital, Birmingham, UK
Phillip Cox, Department of Pathology, Birmingham Women's Hospital, Birmingham, UK
Daniel H Cohn, David L Rimoin, Ralph S Lachman, Medical Genetics Institute, Cedars-Sinai Medical Center, Los Angeles, California, USA
Bronwyn Kerr, Academic Unit of Medical Genetics and Regional Genetic Service, Central Manchester and Manchester Children's Hospitals University NHS Trust, Manchester, UK
Sheila Unger, Andrea Superti-Furga, Centre for Pediatrics and Adolescent Medicine, Freiburg University Hospital, Freiburg, Germany
Hirofumi Ohashi, Division of Medical Genetics, Saitama Children's Medical Center, Iwatsuki, Japan

Competing interests: None declared.

Correspondence to: Dr S Ikegawa, Laboratory for Bone and Joint Diseases, SNP Research Center, RIKEN, 4-6-1 Shirokanedai, Minato-ku, Tokyo 108-8639, Japan; sikegawa@ims.u-tokyo.ac.jp

Received 8 May 2006
Revised 25 September 2006
Accepted 27 September 2006

REFERENCES

1 **Dror Y**, Freedman MH. Shwachman-Diamond syndrome. *Br J Haematol* 2002;**118**:701–13.
2 **Boocock GR**, Morrison JA, Popovic M, Richards N, Ellis L, Durie PR, Rommens JM. Mutations in SBDS are associated with Shwachman-Diamond syndrome. *Nat Genet* 2003;**33**:97–101.
3 **Savchenko A**, Krogan N, Cort JR, Evdokimova E, Lew JM, Yee AA, Sanchez-Pulido L, Andrade MA, Bochkarev A, Watson JD, Kennedy MA, Greenblatt J, Hughes T, Arrowsmith CH, Rommens JM, Edwards AM. The Shwachman-Bodian-Diamond syndrome protein family is involved in RNA metabolism. *J Biol Chem* 2005;**280**:19213–20.
4 **Shammas C**, Menne TF, Hilcenko C, Michell SR, Goyenechea B, Boocock GR, Durie PR, Rommens JM, Warren AJ. Structural and mutational analysis of the SBDS protein family: insight into the leukemia-associated Shwachman-Diamond syndrome. *J Biol Chem* 2005;**280**:19221–9.
5 **Mack DR**, Forstner GG, Wilschanski M, Freedman MH, Durie PR. Shwachman syndrome: exocrine pancreatic dysfunction and variable phenotypic expression. *Gastroenterology* 1996;**111**:1593–602.
6 **Cipolli M**, D'Orazio C, Delmarco A, Marchesini C, Miano A, Mastella G. Shwachman's syndrome: pathomorphosis and long-term outcome. *J Pediatr Gastroenterol Nutr* 1999;**29**:265–72.
7 **Ginzberg H**, Shin J, Ellis L, Morrison J, Ip W, Dror Y, Freedman M, Heitlinger LA, Belt MA, Corey M, Rommens JM, Durie PR. Shwachman syndrome: phenotypic manifestations of sibling sets and isolated cases in a large patient cohort are similar. *J Pediatr* 1999;**135**:81–8.
8 **Dror Y**. Shwachman-Diamond syndrome. *Pediatr Blood Cancer* 2005;**45**:892–901.
9 **Hall GW**, Dale P, Dodge JA. Shwachman-Diamond syndrome: UK perspective. *Arch Dis Child* 2006;**91**:521–4.
10 **Danks DM**, Haslam RHA, Mayne V, Kaufmann HJ, Holtzapple PG. Metaphyseal chondrodysplasia, neutropenia, and pancreatic insufficiency presenting with respiratory distress in the neonatal period. *Arch Dis Child* 1976;**51**:697–701.
11 **Sedaghatian MR**. Congenital lethal metaphyseal chondrodysplasia: a newly recognized complex autosomal recessive disorder. *Am J Med Genet* 1980;**6**:269–74.
12 **Nakashima E**, Mabuchi A, Makita Y, Masuno M, Ohashi H, Nishimura G, Ikegawa S. Novel SBDS mutations caused by gene conversion in Japanese patients with Shwachman-Diamond syndrome. *Hum Genet* 2004;**114**:345–8.
13 **Peeden JN Jr**, Rimoin DL, Lachman RS, Dyer ML, Gerard D, Gruber HE. Spondylometaphyseal dysplasia, Sedaghatian type. *Am J Med Genet* 1992;**44**:651–6.
14 **Superti-Furga A**, Unger S, the Nosology Group of the International Skeletal Dysplasia Society. Nosology and classification of genetic skeletal disorders: 2006 revision. *Am J Med Genet* 2007;**143**:1–18.
15 **Spranger JW**, Brill PW, Poznanski A, eds. *Bone dysplasias:an atlas of genetic disorders of skeletal development.*2nd edn. Oxford: Oxford University Press, 2002:109–11.
16 **Kozlowski K**, Morris L. Shwachman's syndrome: unusual presentation as congenital rickets and asphyxiating thoracic dystrophy. *Fortschr Roentgenstr* 1991;**154**:344–5.
17 **Makitie O**, Ellis L, Durie PR, Morrison JA, Sochett EB, Rommens JM, Cole WG. Skeletal phenotype in patients with Shwachman-Diamond syndrome and mutations in SBDS. *Clin Genet* 2004;**65**:101–12.
18 **Opitz JM**, Spranger JW, Stoss HR, Pesch H-J, Azadeh B. Sedaghatian congenital lethal metaphyseal chondrodysplasia--observations in a second Iranian family and histopathological studies. *Am J Med Genet* 1987;**26**:583–90.
19 **Campbell RSD**, Ireland M, Bloxham CA, Chippindale AJ. Platyspondylic lethal osteochondrodysplasia: Shiraz type with radiological–pathological correlation. *Pediatr Radiol* 1992;**22**:90–2.
20 **Elcioglu N**, Hall CM. Spondylometaphyseal dysplasia--Sedaghatian type. *Am J Med Genet* 1998;**76**:410–4.
21 **Kautouby A**, Habibullah J, Moinuddin FA. Spondylometaphyseal dysplasia: Sedaghatian type. *Am J Med Genet* 2000;**90**:199–202.
22 **Foulds N**, Fairhurst J, Temple IK, Cade S, Groves C, Lancaster T. A female case of Sedaghatian type spondylometaphyseal dysplasia. *Am J Med Genet* 2003;**118**:377–81.
23 **Kujpers TW**, Alders M, Tool ATJ, Mellink C, Roos D, Hennekam CM. Hematologic abnormalities in Shwachman Diamond syndrome: lack of genotype–phenotype relationship. *Blood* 2005;**106**:356–61.
24 **Austin KM**, Leary RJ, Shimamura A. The Shwachman-Diamond SBDS protein localizes to the nucleolus. *Blood* 2005;**106**:1253–8.

nature medicine

Nucleotide-sugar transporter SLC35D1 is critical to chondroitin sulfate synthesis in cartilage and skeletal development in mouse and human

Shuichi Hiraoka[1,13], Tatsuya Furuichi[2,13], Gen Nishimura[3], Shunichi Shibata[4], Masaki Yanagishita[5], David L Rimoin[6], Andrea Superti-Furga[7], Peter G Nikkels[8], Minako Ogawa[1], Kayoko Katsuyama[1], Hidenao Toyoda[9–11], Akiko Kinoshita-Toyoda[9,10], Nobuhiro Ishida[12], Kyoichi Isono[1], Yutaka Sanai[12], Daniel H Cohn[6], Haruhiko Koseki[1] & Shiro Ikegawa[2]

Proteoglycans are a family of extracellular macromolecules comprised of glycosaminoglycan chains of a repeated disaccharide linked to a central core protein[1,2]. Proteoglycans have critical roles in chondrogenesis and skeletal development. The glycosaminoglycan chains found in cartilage proteoglycans are primarily composed of chondroitin sulfate[3]. The integrity of chondroitin sulfate chains is important to cartilage proteoglycan function; however, chondroitin sulfate metabolism in mammals remains poorly understood. The solute carrier-35 D1 (SLC35D1) gene (*SLC35D1*) encodes an endoplasmic reticulum nucleotide-sugar transporter (NST) that might transport substrates needed for chondroitin sulfate biosynthesis[4,5]. Here we created *Slc35d1*-deficient mice that develop a lethal form of skeletal dysplasia with severe shortening of limbs and facial structures. Epiphyseal cartilage in homozygous mutant mice showed a decreased proliferating zone with round chondrocytes, scarce matrices and reduced proteoglycan aggregates. These mice had short, sparse chondroitin sulfate chains caused by a defect in chondroitin sulfate biosynthesis. We also identified that loss-of-function mutations in human *SLC35D1* cause Schneckenbecken dysplasia, a severe skeletal dysplasia. Our findings highlight the crucial role of NSTs in proteoglycan function and cartilage metabolism, thus revealing a new paradigm for skeletal disease and glycobiology.

Chondroitin sulfate chains consist of repeating disaccharide units of *N*-acetylgalactosamine (GalNAc) and glucuronic acid (GlcUA), which are sulfated at either the C6 or C4 position of GalNAc[3]. The integrity of the chondroitin sulfate chain is maintained by elongation (biosynthesis) of the chain and by sulfation of GalNAc. It has been suggested that the chondroitin sulfate status of proteoglycan modulates its functions in epiphyseal cartilage. In humans, after skeletal maturation and concurrent with the disappearance of epiphyseal cartilage, chondroitin sulfate chain length decreases by more than half, and the ratio of C6 to C4 sulfation in chondroitin sulfate increases more than 20-fold[6]. These findings suggest that the chondroitin sulfate chain length and sulfation pattern are essential to cartilage growth activity. Accordingly, a broad spectrum of skeletal dysplasias results from mutations causing undersulfation of chondroitin sulfate chains in humans and in mice[2,7–11]. However, the full impact of defective chondroitin sulfate chain length remains unclear, primarily owing to the lack of a mammalian model.

The SLC35 gene family contains at least 17 human genes that encode NSTs[12]. NSTs are multiple-pass membrane-spanning proteins that transport nucleotide-sugars from the cytosol into the lumens of various organelles. Several NSTs are important in glycosaminoglycan synthesis, supplying specific glycosaminoglycans with substrates for biosynthesis[12]. SLC35D1 transports UDP-GlcUA and UDP-GalNAc, which are substrates for the synthesis of chondroitin sulfate disaccharide repeats[4,5]. This transporter activity suggests that SLC35D1 is involved in chondroitin sulfate biosynthesis; however, much remains to be learned about the biological role of SLC35D1 in chondroitin sulfate biosynthesis.

[1]Laboratory for Developmental Genetics, RIKEN Research Center for Allergy and Immunology, 1-7-22 Suehirocho, Tsurumi-ku, Yokohama, Kanagawa 230-0045, Japan. [2]Laboratory of Bone and Joint Diseases, Single Nucleotide Polymorphism Research Center, RIKEN, 4-6-1 Shirokanedai, Minato-ku, Tokyo 108-8639, Japan. [3]Department of Radiology, Tokyo Metropolitan Kiyose Children's Hospital, 1-3-1 Umezono, Kiyose 204-8567, Japan. [4]Maxillofacial Anatomy, Department of Maxillofacial Biology, and [5]Biochemistry, Department of Hard Tissue Engineering, Division of Biomatrix, Graduate School, Tokyo Medical and Dental University, 1-5-45 Yushima, Bunkyo-ku, Tokyo 113-8549, Japan. [6]Medical Genetics Institute, Cedars-Sinai Medical Center, SSB-3, 8700 Beverly Blvd., and Departments of Human Genetics and Pediatrics, David Geffen School of Medicine at UCLA, Los Angeles, California 90048, USA. [7]Centre for Paediatrics and Adolescent Medicine, Freiburg University Hospital, Mathildenstrasse 1, D-79106 Freiburg, Germany. [8]Department of Pathology, H04.312 University Medical Center Utrecht Postbox 85500, 3508 GA Utrecht, The Netherlands. [9]Faculty of Pharmaceutical Sciences, Chiba University, 1-33, Yayoi, Inage, Chiba 263-8522, Japan. [10]Core Research for Evolutional Science and Technology and [11]Precursory Research for Embryonic Science and Technology, Japan Science and Technology Agency, 4-1-8 Honcho, Kawaguchi, Saitama 332-0012, Japan. [12]Department of Biochemical Cell Research, Tokyo Metropolitan Institute of Medical Science, 3-18-22 Honkomagome, Bunkyo-ku, Tokyo 113-8613, Japan. [13]These authors contributed equally to this work. Correspondence should be addressed to H.K. (koseki@rcai.riken.jp) or S.I. (sikegawa@ims.u-tokyo.ac.jp).

Received 30 April; accepted 21 August; published online 21 October 2007; doi:10.1038/nm1655

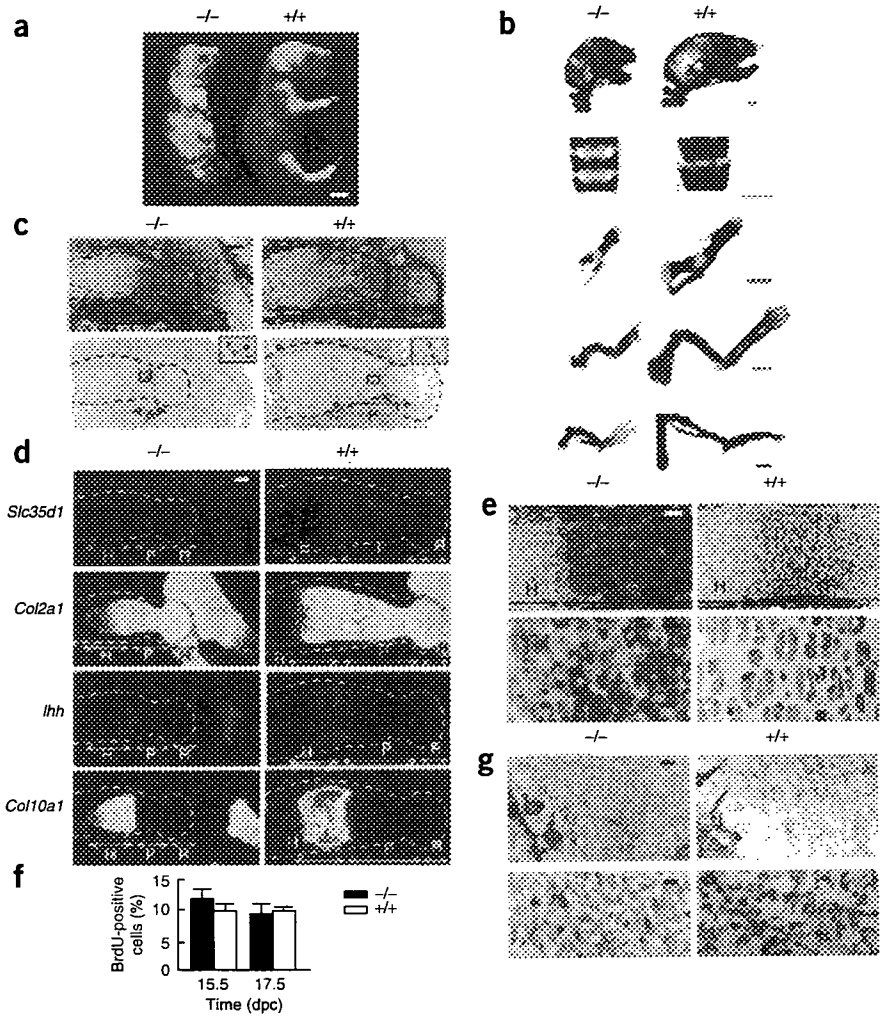

Figure 1 Phenotype of the *Slc35d1*-deficient mice. (**a**) Gross morphology of wild-type (+/+) and *Slc35d1*$^{-/-}$ (-/-) mice at newborn stage. Scale bar, 5 mm. (**b**) Skeletal preparations of 18.5-dpc embryos stained with Alcian blue and Alizarin red. From the top, skull, lumbar spine, ilium, forelimb and hindlimb are shown. Scale bars, 1 mm. (**c–g**) Histological analysis of the epiphyseal cartilage of wild-type and *Slc35d1*$^{-/-}$ embryos. Dashed lines define the humerus. Resting (R), proliferating (P) and hypertrophic (H) zones in the epiphyseal cartilage are demarcated. (**c**) Definition of the proliferating zone by BrdU incorporation. H&E staining (top) and immunostaining with antibody to BrdU (bottom) of the epiphyseal cartilage from BrdU-labeled embryos at 15.5 dpc. Insets at upper right of the lower panels show BrdU-positive cells in the boxed regions. Scale bar, 200 μm. (**d**) *In situ* hybridization to determine the expression of *Slc35d1* and zone-specific molecular marker mRNA in the epiphyseal cartilage of 15.5 dpc embryos. In wild-type cartilage, *Slc35d1* was preferentially expressed in proliferating zones. *Ihh* and *Col10a1* were expressed in prehypertrophic and hypertrophic zones, respectively, whereas *Col2a1* was preferentially expressed in resting and proliferating zones. Expression patterns of the zonal markers were not markedly affected in *Slc35d1*$^{-/-}$ mice. Scale bar, 200 μm. (**e**) H&E staining of the epiphyseal cartilage of 15.5-dpc embryos (top) and toluidine blue staining of plastic sections of the proliferating zone of the epiphyseal cartilage from 15.5-dpc embryos (bottom). Scale bars, 100 μm (top) and 10 μm (bottom). (**f**) Frequency of BrdU-positive cells in the proliferating zone of the epiphyseal cartilage of embryos at 15.5 and 17.5 dpc. The number of BrdU-positive cells and the total number of cells in five sections are from two mice. Values represent mean ± s.e.m. (**g**) Electron microscopic images of ECM from the proliferating zone of the epiphyseal cartilage of 17.5-dpc embryos magnified 10,000× (top) and 300,000× (bottom). A chondrocyte was observed in the lower left corner of the top micrograph. Scale bars, 1 μm (top) and 0.1 μm (bottom).

To clarify the biological role of SLC35D1, we isolated a full-length mouse *Slc35d1* messenger RNA and synthesized its complementary DNA. Its deduced amino acid sequence was 97% identical to that of human SLC35D1. The mouse Slc35d1 protein had substrate specificity and subcellular localization identical to those of its human counterpart (**Supplementary Fig. 1** online). Then we established an *Slc35d1*$^{+/-}$ mouse line that transmits the mutation through the germline (**Supplementary Fig. 2** online). These heterozygous mice showed no phenotypic abnormalities. RT-PCR analysis confirmed the absence of *Slc35d1* transcripts in homozygous embryos. *Slc35d1*$^{-/-}$ mice did not survive the neonatal period; their crown-rump length was reduced and their limbs were extremely short (**Fig. 1a**). Other external phenotypic traits included a short snout, protruding tongue, narrow thorax and protruding abdomen. Skeletal preparations showed hypoplasia of craniofacial bones, flattening of vertebral bodies, longitudinally short ilia and extremely short long bones (**Fig. 1b**). This severe chondrodysplasia confirms that Slc35d1 is crucial during prenatal skeletal development in mice.

To understand the pathogenic basis of the chondrodysplasia phenotype, we investigated the histology of the epiphyseal cartilage of *Slc35d1*$^{-/-}$ mice at 15.5 days post coitus (dpc). Consistent with the shortened limb length, the proliferating zone, as defined by BrdU incorporation, was greatly reduced (**Fig. 1c**). *Slc35d1* expression was intense in the proliferating zone of wild-type but absent in mutant mice (**Fig. 1d**). The *Slc35d1*$^{-/-}$ epiphyseal cartilage showed a disorganized proliferating zone in which the normal columnar alignment of chondrocytes was replaced by closely packed, round chondrocytes and very little extracellular matrix (ECM) space (**Fig. 1e**). The frequency of BrdU-positive cells in the proliferating zone of the mutant mice was similar to that in the wild-type mice (**Fig. 1f**), and TUNEL-positive cells were rarely observed in the proliferating zones of both mutant and wild-type mice (data not shown). The expression patterns of the zone-specific markers *Col2a1*, *Ihh* and *Col10a1* in *Slc35d1*$^{-/-}$ mice were similar to those in wild-type mice (**Fig. 1d**), indicating that the pattern of chondrocyte differentiation was not affected. Electron microscopic analysis of the ECM from the proliferating zones of *Slc35d1*$^{-/-}$ mice showed a loss of the pericellular halo and a denser collagen fibril network (**Fig. 1g**). Higher-magnification images revealed a severe reduction in and amorphous appearance of proteoglycan aggregates (**Fig. 1g**). These findings suggest that proteoglycan synthesis is impaired in *Slc35d1*$^{-/-}$ epiphyseal cartilage.

To characterize abnormal proteoglycan metabolism in the mutant, we examined the distribution of the core protein of aggrecan, a major component of cartilage proteoglycan, and the chondroitin sulfate and

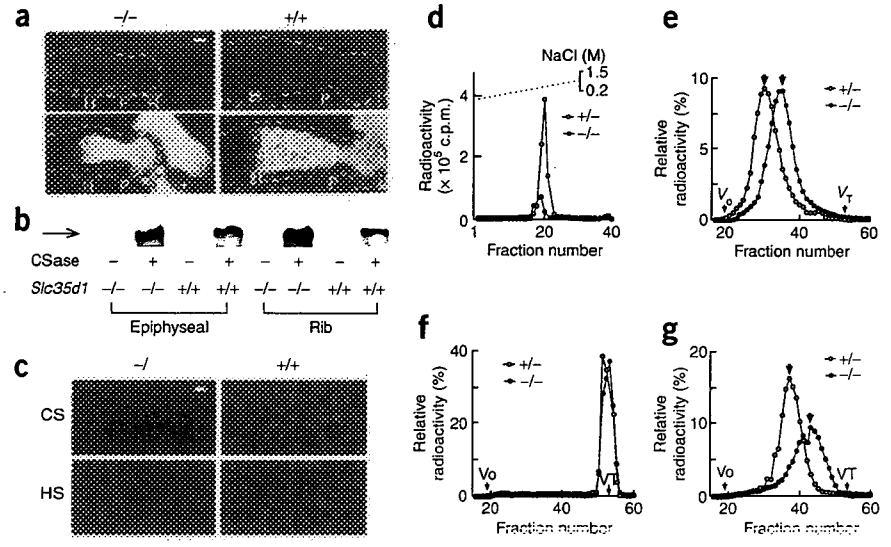

Figure 2 Effects of impaired chondroitin sulfate synthesis on cartilage proteoglycan in *Slc35d1*-deficient mice. (**a**) Immunostaining and *in situ* hybridization analysis for the core protein of aggrecan. Sections from the distal humerus of wild-type (+/+) and *Slc35d1*$^{-/-}$ (-/-) embryos at 15.5 dpc are shown. Dashed lines define the humerus. Zones are indicated as in **Figure 1**. Scale bar, 200 μm. Staining with an antibody to an aggrecan core protein (top) and *in situ* hybridization for the expression of *Agc1* mRNA (bottom) are shown. (**b**) Western blot for aggrecan core protein in the epiphyseal and rib cartilages of 17.5-dpc embryos. The intact aggrecan core polypeptide, with a molecular mass of ~220 kDa (arrow), is visible only after chondroitinase (CSase) treatment in wild-type and homozygote cartilage. (**c**) Staining with antibodies to chondroitin mimotope (CS, top) and heparan sulfate (HS, bottom). Sections from the proliferating zone of the epiphyseal cartilage of 15.5-dpc embryos are used. Scale bar, 10 μm. (**d–g**) Glycosaminoglycan synthesis in cartilage explants. Glycosaminoglycans of proteoglycans in rib-cartilage explants were metabolically labeled with [^{35}S]sulfate for subsequent chromatographic analysis. Open and closed circles indicate samples from *Slc35d1*$^{+/-}$ and *Slc35d1*$^{-/-}$, respectively. Radioactivity is indicated as absolute (**d**) and as relative value (%) as compared to the total analyzed sample (**e–g**). (**d**) Purification of the proteoglycan fraction. Explant extracts were fractionated by Q-Sepharose chromatography and peak fractions were pooled (proteoglycan fraction). Aliquots were used for the following chromatography experiments. (**e**) Sephacryl S-500HR chromatography with untreated samples. The peak positions of *Slc35d1*$^{-/-}$ and *Slc35d1*$^{+/-}$ (arrows) corresponded to dextran of 3.1 × 10^5 kDa and 1.2 × 10^6 kDa, respectively. V_o, exclusion volume of the column; V_t, total volume of the column. (**f**) Superose6 chromatography with samples digested with chondroitinase ABC. (**g**) Superose6 chromatography for glycosaminoglycan analysis. Before loading, the glycosaminoglycans were released from the proteoglycan core proteins by β-elimination. The peak positions of *Slc35d1*$^{-/-}$ and *Slc35d1*$^{+/-}$ (arrows) corresponded to chondroitin sulfate chains of 1.3 × 10^4 kDa and 2.7 × 10^4 kDa, respectively.

heparan sulfate contents in epiphyseal cartilage. Immunostaining and *in situ* hybridization analysis revealed that the amount of aggrecan core did not differ between *Slc35d1*$^{-/-}$ and wild-type mice (**Fig. 2a**). These results were further confirmed by western blot analysis (**Fig. 2b**). Immunohistological studies of chondroitin sulfate and heparan sulfate distribution suggested that the chondroitin sulfate content of the *Slc35d1*$^{-/-}$ epiphyseal cartilage was markedly reduced, whereas the heparan sulfate content was unaltered (**Fig. 2c**). Disaccharide compositional analysis[13] also showed that chondroitin sulfate abundance in the *Slc35d1*$^{-/-}$ cartilage at 18.5 dpc decreased to one-seventh that of the wild type, but heparan sulfate abundance did not change (**Supplementary Table 1** online). These results suggest that the *Slc35d1* mutation causes defects in the chondroitin sulfate biosynthesis of cartilage proteoglycan core proteins.

We further investigated the effects of altered chondroitin sulfate biosynthesis on proteoglycans in *Slc35d1*$^{-/-}$ embryos by labeling newly synthesized chondroitin sulfate with [^{35}S]sulfate in explant cultures of rib cartilage[14]. The radioactivity of the proteoglycan fraction per explant weight in *Slc35d1*$^{-/-}$ mice was reduced to one-third of that in heterozygotic mice, as determined by ion-exchange chromatography (**Fig. 2d**). We next examined the relative molecular mass of proteoglycans by using gel-filtration chromatography. The peak radioactivity in the homozygous mouse extract shifted five fractions toward the total volume of the column (V_T) relative to the heterozygous mouse extract peak. This shift represents a 75% decrease in the average proteoglycan molecular mass in *Slc35d1*$^{-/-}$ extracts (**Fig. 2e**). We confirmed that these radioactive peaks represent chondroitin sulfate by digesting the extract with chondroitinase ABC, which shifted the peaks completely to the V_T (**Fig. 2f**). Finally, we measured chondroitin sulfate chain length by releasing chondroitin sulfate chains from proteoglycan core proteins through β-elimination. In *Slc35d1*$^{-/-}$ extracts, the major radioactive peak was broad, split and shifted to a lower-molecular-mass position (**Fig. 2g**), indicating a reduction in *Slc35d1*$^{-/-}$ cartilage chondroitin sulfate chain length to half of that of the heterozygote. These results indicate that chondroitin sulfate biosynthesis is impaired in *Slc35d1*$^{-/-}$ cartilage.

Schneckenbecken dysplasia (OMIM 269250) is a perinatally lethal skeletal dysplasia that is inherited as an autosomal recessive trait[15–17]. The German term 'Schneckenbecken' refers to the distinctive, snail-like appearance of the ilia that results from a medial bone projection from the inner iliac margin. Other hallmarks of Schneckenbecken dysplasia include thoracic hypoplasia, severe flattening of the vertebral bodies and short, thick long bones. The similarities of the skeletal and histological findings in *Slc35d1*$^{-/-}$ mice to the Schneckenbecken dysplasia phenotype prompted us to search for *SLC35D1* mutations in individuals with Schneckenbecken dysplasia (**Supplementary Table 2** online). In two subjects with typical Schneckenbecken dysplasia (**Supplementary Case Report** online), we found mutations in both alleles (**Fig. 3a**). Subject 1, the product of a consanguineous marriage, was homozygous for a 1–base pair deletion (c.125delA) in exon 1 that produced a premature stop codon (p.S42fsX9). Subject 2 was compound heterozygous for a nonsense mutation in exon 11, c.932G→A (p.W311X) and a splice–donor site mutation, IVS7+1G → T. Sequencing of the RT-PCR product derived from Subject 2 revealed that the IVS7+1G→T mutation causes abnormal splicing, which produces a premature stop codon (**Fig. 3b**). The predicted truncated protein (p.K212insLSSNLKLX) lacks the C-terminal 143 amino acids of SLC35D1 and contains 7 substituted amino acids. Thus, all three mutations are predicted to produce truncated proteins.

Next, we evaluated the NST activity of the predicted SLC35D1 truncation proteins in Subject 2 by using a yeast complementation assay[4,5]. Western blot analysis confirmed the expression of the mutant and wild-type SLC35D1 in microsome fractions prepared from transfected yeast cells (**Fig. 3c**). Although SLC35D1-expressing microsomes

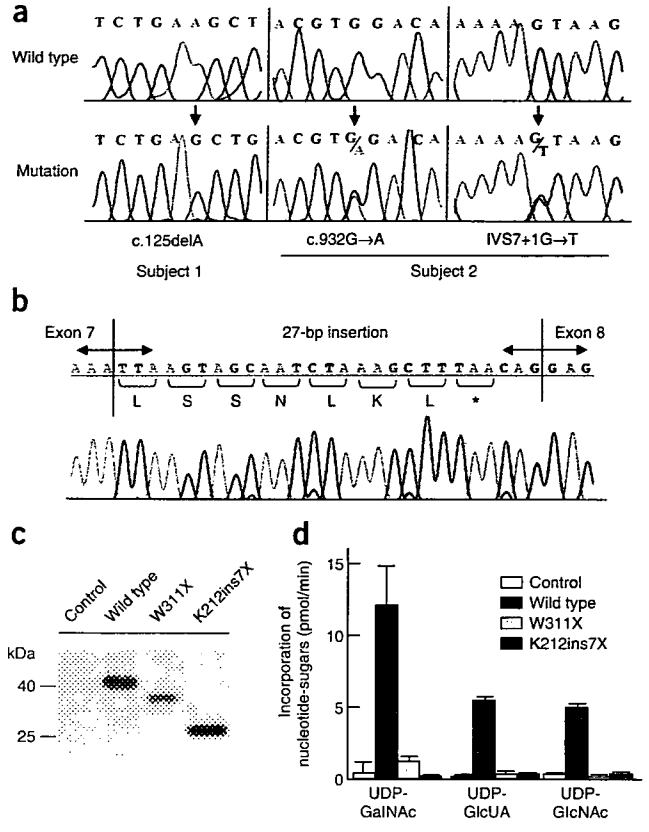

Figure 3 Loss-of-function mutations of *SLC35D1* in Schneckenbecken dysplasia. **(a)** Identification of *SLC35D1* mutations in two patients with typical Schneckenbecken dysplasia. Top schematic shows wild-type sequence and lower schematic mutant sequence. Mutations are indicated by arrows. These mutations were not found in more than 40 ethnicity-matched controls or in public sequence-variation databases. **(b)** Abnormal RNA splicing caused by the IVS7+1G→T mutation in Subject 2. Sequencing of the RT-PCR product encompassing exons 5–9 of RNA from Subject 2 showed an in-frame insertion of 27 nucleotides between exons 7 and 8 (c.636_637 ins27), which produced a premature stop codon. **(c,d)** Loss of nucleotide-sugar transporter activity by mutant SLC35D1 proteins. Microsomes were prepared from yeast cells transfected with empty vector, SLC35D1 or its mutant expression vector. **(c)** Western blots for wild-type and mutant SLC35D1 proteins in yeast microsomes. **(d)** Transporter activities of the mutant SLC35D1 proteins. The incorporation of nucleotide-sugars for 1 min at 30 °C per mg microsome protein is shown. Each value represents the mean ± s.d. of duplicate experiments.

showed higher incorporation of UDP-GalNAc, UDP-GlcUA and UDP-GlcNAc relative to a non-expressing control, those expressing either truncated protein showed the same incorporation levels as the control (**Fig. 3d**). Therefore, both mutant proteins in Subject 2 completely lack NST activity; judging from the considerably shorter length of p.S42fsX9 in Subject 1 (**Supplementary Fig. 3** online), this mutant should also lose activity. These findings indicate that Schneckenbecken dysplasia can be caused by loss of SLC35D1 function.

Thus, we have shown that SLC35D1 has an indispensable role in mouse and human skeletal formation. SLC35D1 deficiency causes the shortening of chondroitin sulfate chains, leading to the disorganization of a functional ECM in epiphyseal cartilage and to skeletal dysplasias. SLC35D1 is a crucial molecule that regulates the chondroitin sulfate length in cartilage proteoglycan by supplying the nucleotide-sugars used as substrates for chondroitin sulfate biosynthesis. Notably, the reduction in the average molecular mass of proteoglycan in the *Slc35d1*$^{-/-}$ cartilage was discordant with that of chondroitin sulfate, as determined by gel-filtration chromatography (**Fig. 2e,g**). These results suggest that not only is the chain length reduced, but so is the number of chondroitin sulfate chains on the aggrecan core in *Slc35d1*$^{-/-}$ mice. SLC35D1 may be involved in both the initiation and the elongation of chondroitin sulfate chain synthesis. Further studies are required to evaluate this possibility.

Our identification of the *SLC35D1* mutation in Schneckenbecken dysplasia contributes to the molecular classification and diagnosis of perinatally lethal skeletal dysplasias. Human skeletal dysplasias are grouped by their phenotypic similarities, which reflect causal similarity in many cases[18]. Schneckenbecken dysplasia belongs to the 'severe spondylodysplastic dysplasias' group, for which no causative mutations were known before this study. *SLC35D1* and other genes acting in the same genetic pathway may well be responsible for these lethal skeletal dysplasias. Also, our findings underscore other NSTs as new candidates for human skeletal dysplasias. Indeed, a missense mutation in the bovine *Slc35a3* gene, which encodes a UDP-GlcNAc transporter, is known to be responsible for complex vertebral malformations[19]. Our study may help build new bridges between skeletal biology and glycobiology.

METHODS

Generation of *Slc35d1*-deficient mice. We generated a knockout mouse line of the *Slc35d1* gene by using methods previously described[20]. A bacterial artificial chromosome (BAC) clone containing the mouse *Slc35d1* was screened from an embryonic stem (ES) cell–BAC library (see Acknowledgments). Using the BAC, we constructed a targeting vector to eliminate the genomic region encompassing exons 1–3 (**Supplementary Fig. 2**). We introduced this vector into R1 ES cells and cloned homologous recombinants through selection with antibiotics and verification of the genotype. We developed chimeric mice with the targeted ES-cell clones and obtained homozygous mice by interbreeding the offspring. All procedures, including mouse handling, were conducted according to guidelines approved by the RIKEN Institutional Animal Care and Use Committee.

Skeletal histology, *in situ* hybridization and immunohistological analysis. We stained bone and cartilage from 18.5 dpc embryos with Alizarin red and Alcian blue as described previously[21]. We prepared paraffin sections (5 μm) processed from 15.5 dpc embryos for H&E staining, *in situ* hybridization and immunohistochemistry. We performed *in situ* hybridizations as previously described[22], using radiolabeled antisense RNA for *Slc35d1*, *Col2a1*, *Ihh*, *Col10a1* and *Agc1*. We performed immunohistological detection of aggrecan core protein and chondroitin mimotope as described elsewhere[23], using specimens pretreated with chondroitinase ABC. We immunodetected heparan sulfate with a heparan sulfate–specific antibody, 10E4 (Seikagaku Corporation). We labeled proliferating cells in 15.5- and 17.5-dpc embryos with BrdU (Sigma-Aldrich Japan) and immunodetected them with antibody to BrdU (clone B44; Nippon Becton Dickinson) as described previously[24].

Transmission electron microscopy. For ultrastructural analysis, we fixed specimens of epiphyseal cartilage taken from the humerus of 17.5-dpc embryos through a 1-d immersion in a 5% (w/v) glutaraldehyde and 4% (w/v) paraformaldehyde solution and a subsequent 3-h soak in 1% (w/v) osmium tetroxide. We embedded specimens in Epon 812 (TAAB) and examined ultrathin sections with the HITACHI H-800 transmission electron microscope (Hitachi).

Western blot analysis. We extracted cartilage protein from 17.5-dpc embryos with 4 M guanidine hydrochloride. We exchanged the guanidine hydrochloride in the extracts to 8 M urea and 0.5% polyoxyethylene(10) lauryl ether, and then removed the urea by dialysis. Subsequently, we digested the samples, equivalent to 5 μg of protein, with 0.01 unit of chondroitinase ABC (Seikagaku Corporation) and analyzed by western blotting with antibodies to the aggrecan core peptide (CHEMICON International).

Analysis of glycosaminoglycan synthesis in cartilage explant. We analyzed glycosaminoglycan synthesis in cartilage explants as previously described[14], except that we used a Sephacryl S500HR column whose length and diameter were 30 cm and 1 cm, respectively (GE Healthcare) in **Figure 2e**. We cultured rib cartilage from three embryos at 18.5 dpc in DMEM with [^{35}S]sulfate (GE Healthcare) to label the glycosaminoglycan sulfate residues. Proteoglycan fractions were obtained from cultures through extraction with 4 M guanidine hydrochloride and purification by Q-Sepharose (GE Healthcare) column chromatography. We then measured the molecular size of proteoglycan and glycosaminoglycan in the proteoglycan fractions with gel-filtration chromatography.

Disaccharide compositional analysis. We prepared lyophilized humerus and femur for disaccharide compositional analysis. After exhaustive enzymatic digestion of partially purified glycosaminoglycans with a mixture of chondroitinase and heparitinase, we determined the unsaturated disaccharide composition by fluorometric postcolumn HPLC[13] with chondroitin sulfate- (Seikagaku Corporation) and heparan sulfate–derived (Sigma-Aldrich) unsaturated disaccharide standards.

Human subjects. We screened for *SLC35D1* mutations in six individuals with Schneckenbecken dysplasia who were registered in the International Skeletal Dysplasia Registry, the European Sustainable Development Network and the Japanese Skeletal Dysplasia Consortium; three had typical and three had possible Schneckenbecken dysplasia (**Supplementary Table 2**). Samples were obtained after informed consent. All procedures were conducted according to the protocols and guidelines approved by the participating institutions. Brief summaries of the findings in the two subjects with *SLC35D1* mutations are provided in the **Supplementary Case Report**.

Mutation screening. We isolated genomic DNAs by using standard procedures and examined *SLC35D1* for mutations by PCR from genomic DNA followed by direct sequencing. We amplified the 12 exons of *SLC35D1* with their flanking intron sequences by PCR and sequenced the products with an ABI Prism 3700 automated sequencer (PE Biosystems). PCR conditions and primer sequences are available upon request.

RT-PCR analysis. We extracted total RNA from the frozen chondro-osseous tissue of Subject 2 by using ISOGEN (Nippongene) and synthesized random-primed cDNAs with the TaqMan Multiscribe Reverse kit (Applied Biosystems). To examine the effect of the IVS7+1G→T mutation on RNA splicing, we amplified a *SLC35D1* cDNA segment spanning exons 5–9 with the primer pair 5′-TCTGAGAAGGTTCTCCATCC-3′ and 5′-AGAAGAAAGAGGGTGTCAGC-3′. To examine whether mutations in Subject 2 were compound heterozygous, we amplified a cDNA segment spanning exons 7–12 with the primer pair 5′-TTGGCATTTGATCTGGAAGGA-3′ and 5′-TATACCAGGCTCCCAGCAAT-3′. We subcloned RT-PCR products with the TOPO TA Cloning Kit (Invitrogen) and sequenced them.

Nucleotide-sugar transporter activity. We measured the NST activity of SLC35D1 mutants with a heterologous expression system in *Saccharomyces cerevisiae* as previously described[4,5]. We constructed pYEX-BESN3 expression vectors encoding N-terminal hemagglutinin epitope–tagged wild-type and mutant SLC35D1 proteins. We prepared microsome fractions from cells expressing wild-type and mutant SLC35D1 and measured the amount of radiolabeled nucleotide-sugar incorporated into the fractions.

Note: Supplementary information is available on the Nature Medicine website.

ACKNOWLEDGMENTS

We thank M. Nakayama (Kazusa DNA Research Institute) for donating the ES cell–BAC library. We are grateful to M. Muraoka for measurement of NST activity, to I. Kataoka and Y. Mizutani-Koseki for their assistance in histochemical analysis and *in situ* hybridization and to S. Tominaga for her help in genetic analysis of the human *SLC35D1*. This project was supported by Special Coordination Funds for the Promotion of Science and Technology from the Japanese Ministry of Education, Culture, Sports, Science and Technology (Contract Grant No. 13043003 to H.K.) and by grants-in-aid from the Ministry of Education, Culture, Sports and Science of Japan (Contract Grant No. 19209049), Research on Child Health and Development (Contract Grant Nos. 17C-1 and H18-005 to S.I.), the Ministry of Education, Culture, Sports and Science of Japan (Contract Grant No. 19510205 to S.H.) and the US National Institutes of Health (HD22657 and MO1-RR00425 to D.H.C. and D.L.R.). D.H.C. is the recipient of a Winnick Family Clinical Scholar Award.

AUTHOR CONTRIBUTIONS

S.H. and T.F. performed the main experiments, analyzed data and prepared the manuscript. G.N., D.L.R., A.S.-F., P.G.N. and D.H.C. recruited human subjects and analyzed the human phenotypic data. S.S. and M.Y. performed proteoglycan analysis in knockout mice. M.O. and K.K. generated knockout mice and carried out histological analysis. H.T. and A.K.-T. determined glycosaminoglycan content. N.I., K.I. and Y.S. assayed mouse Slc35d1 protein. H.K. and S.I. planned and supervised the mouse and human parts of the project, respectively.

Published online at http://www.nature.com/naturemedicine
Reprints and permissions information is available online at http://npg.nature.com/reprintsandpermissions

1. Knudson, C.B. & Knudson, W. Cartilage proteoglycans. *Semin. Cell Dev. Biol.* **12**, 69–78 (2001).
2. Schwartz, N.B. & Domowicz, M. Chondrodysplasias due to proteoglycan defects. *Glycobiology* **12**, 57R–68R (2002).
3. Sugahara, K. & Kitagawa, H. Recent advances in the study of the biosynthesis and functions of sulfated glycosaminoglycans. *Curr. Opin. Struct. Biol.* **10**, 518–527 (2000).
4. Muraoka, M., Kawakita, M. & Ishida, N. Molecular characterization of human UDP-glucuronic acid/UDP-N-acetylgalactosamine transporter, a novel nucleotide sugar transporter with dual substrate specificity. *FEBS Lett.* **495**, 87–93 (2001).
5. Muraoka, M., Miki, T., Ishida, N., Hara, T. & Kawakita, M. Variety of nucleotide sugar transporters with respect to the interaction with nucleoside mono- and diphosphates. *J. Biol. Chem.* **282**, 24615–24622 (2007).
6. Plaas, A.H., Wong-Palms, S., Roughley, P.J., Midura, R.J. & Hascall, V.C. Chemical and immunological assay of the nonreducing terminal residues of chondroitin sulfate from human aggrecan. *J. Biol. Chem.* **272**, 20603–20610 (1997).
7. Superti-Furga, A. *et al.* Achondrogenesis type IB is caused by mutations in the diastrophic dysplasia sulphate transporter gene. *Nat. Genet.* **12**, 100–102 (1996).
8. Hastbacka, J. *et al.* Atelosteogenesis type II is caused by mutations in the diastrophic dysplasia sulfate transporter gene (DTDST): evidence for a phenotypic series involving three chondrodysplasias. *Am. J. Hum. Genet.* **58**, 255–262 (1996).
9. ul Haque, M.F. *et al.* Mutations in orthologous genes in human spondyloepimetaphyseal dysplasia and the brachymorphic mouse. *Nat. Genet.* **20**, 157–162 (1998).
10. Thiele, H. *et al.* Loss of chondroitin 6-*O*-sulfotransferase-1 function results in severe human chondrodysplasia with progressive spinal involvement. *Proc. Natl. Acad. Sci. USA* **101**, 10155–10160 (2004).
11. Kluppel, M., Wight, T.N., Chan, C., Hinek, A. & Wrana, J.L. Maintenance of chondroitin sulfation balance by chondroitin-4-sulfotransferase 1 is required for chondrocyte development and growth factor signaling during cartilage morphogenesis. *Development* **132**, 3989–4003 (2005).
12. Ishida, N. & Kawakita, M. Molecular physiology and pathology of the nucleotide sugar transporter family (SLC35). *Pflugers Arch.* **447**, 768–775 (2004).
13. Toyoda, H., Kinoshita-Toyoda, A. & Selleck, S.B. Structural analysis of glycosaminoglycans in *Drosophila* and *Caenorhabditis elegans* and demonstration that tout-velu, a *Drosophila* gene related to EXT tumor suppressors, affects heparan sulfate *in vivo*. *J. Biol. Chem.* **275**, 2269–2275 (2000).
14. Ogihara, Y. *et al.* Biosynthesis of proteoglycan in bone and cartilage of parathyroid hormone–related protein knockout mice. *J. Bone Miner. Metab.* **19**, 4–12 (2001).
15. Borochowitz, Z. *et al.* A distinct lethal neonatal chondrodysplasia with snail-like pelvis: Schneckenbecken dysplasia. *Am. J. Med. Genet.* **25**, 47–59 (1986).
16. Giedion, A. *et al.* Case report 693. *Skeletal Radiol.* **20**, 534–538 (1991).
17. Nikkels, P.G., Stigter, R.H., Knol, I.E. & van der Harten, H.J. Schneckenbecken dysplasia, radiology and histology. *Pediatr. Radiol.* **31**, 27–30 (2001).
18. Superti-Furga, A. & Unger, S. Nosology and classification of genetic skeletal disorders: 2006 revision. *Am. J. Med. Genet. A.* **143**, 1–18 (2007).
19. Thomsen, B. *et al.* A missense mutation in the bovine SLC35A3 gene, encoding a UDP-N-acetylglucosamine transporter, causes complex vertebral malformation. *Genome Res.* **16**, 97–105 (2006).
20. Joyner, A.L. *Gene Targeting* 1–146 (Oxford University Press, Oxford, UK, 1992).
21. Kessel, M. & Gruss, P. Homeotic transformations of murine vertebrae and concomitant alteration of Hox codes induced by retinoic acid. *Cell* **67**, 89–104 (1991).
22. Kessel, M. & Gruss, P. Murine developmental control genes. *Science* **249**, 374–379 (1990).
23. Shibata, S., Fukada, K., Imai, H., Abe, T. & Yamashita, Y. *In situ* hybridization and immunohistochemistry of versican, aggrecan and link protein, and histochemistry of hyaluronan in the developing mouse limb bud cartilage. *J. Anat.* **203**, 425–432 (2003).
24. Wallin, J. *et al.* The role of Pax-1 in axial skeleton development. *Development* **120**, 1109–1121 (1994).

Hum Genet (2007) 121:625–629
DOI 10.1007/s00439-007-0354-y

ORIGINAL INVESTIGATION

A recurrent mutation in type II collagen gene causes Legg-Calvé-Perthes disease in a Japanese family

Yoshinari Miyamoto · Tatsuo Matsuda · Hiroshi Kitoh · Nobuhiko Haga · Hirofumi Ohashi · Gen Nishimura · Shiro Ikegawa

Received: 31 January 2007 / Accepted: 8 March 2007 / Published online: 30 March 2007

Abstract Legg-Calvé-Perthes disease (LCPD) is a common childhood hip disorder characterized by sequential stages of involvement of the capital femoral epiphyses, including subchondral fracture, fragmentation, re-ossification and healing with residual deformity. Most cases are sporadic, but familial cases have been described, with some families having multiple affected members. Genetic factors have been implicated in the etiology of LCPD, but the causal gene has not been identified. We have located a missense mutation (p.G1170S) in the type II collagen gene (*COL2A1*) in a Japanese family with an autosomal dominant hip disorder manifesting as LCPD and showing considerable intra-familial phenotypic variation. This is the first report of a mutation in hereditary LCPD. *COL2A1* mutations may be more common in LCPD patients than currently thought, particularly in familial and/or bilateral cases.

Y. Miyamoto · S. Ikegawa (✉)
Laboratory for Bone and Joint Diseases,
SNP Research Center, RIKEN,
4-6-1 Shirokanedai, Minato-ku,
Tokyo 108-8639, Japan
e-mail: sikegawa@ims.u-tokyo.ac.jp

T. Matsuda
Department of Orthopedic Surgery,
Tokyo Kosei Nenkin Hospital, Tokyo, Japan

H. Kitoh
Department of Orthopaedic Surgery,
Nagoya University School of Medicine, Nagoya, Japan

N. Haga
Department of Rehabilitation Medicine,
Graduate School of Medicine,
The University of Tokyo, Tokyo, Japan

H. Ohashi
Division of Medical Genetics and Division
of Endocrinology and Metabolism,
Saitama Children's Medical Center, Iwatsuki, Japan

G. Nishimura
Department of Radiology, Tokyo Metropolitan
Kiyose Children's Hospital, Kiyose, Tokyo, Japan

Introduction

Legg-Calvé-Perthes disease (LCPD; OMIM 150600) is a common hip disorder in children. Its annual incidence has been estimated at 0.2–29 per 100,000 in children under age 14 years (Pillai et al. 2005; Rowe et al. 2005). Its peak incidence occurs between the ages of 4 and 8 years, with 10% of cases showing bilateral involvement. Affected children typically present with limping, decreased motion and hip pain (Thompson et al. 2002). Severely affected patients retain deformity of the femoral head in adulthood, typically presenting as coxa plana, and require arthroplasty for treatment of osteoarthritis.

LCPD is considered an idiopathic form of avascular necrosis of the femoral head (ANFH; OMIM 608805) in growing children. ANFH arises as a consequence of a variety of disorders, most commonly trauma, developmental dysplasia of the hip, slipped capital femoral epiphysis, hematological disorders, collagen vascular diseases, corticosteroid usage, hereditary skeletal dysplasias such as multiple epiphyseal dysplasia (Mackenzie et al. 1989) and, more rarely, idiopathic origins. However, the disease process for LCPD is so distinctive that it can be differentiated easily from the other form of ANFH. LCPD progresses through four distinctive stages: (1) growth disturbance, (2) subchondral fracture and fragmentation, (3) re-ossification and (4) healed or residual. These stages of deterioration and

regeneration are cyclic; thus, LCPD is a self-limiting and self-healing disorder, while other forms of ANFH are not.

The precise etiology of LCPD has not been elucidated. Although the factor V Leiden (Gruppo et al. 1998) and the functional variants of β fibrinogen (Dilley et al. 2003) are reported to be associated with LCPD, most cases are idiopathic. Associated factors include deprivation (Margetts et al. 2001), abnormal clotting mechanism (Glueck et al. 1996), smoke exposure (Glueck et al. 1998) and genetic predisposition. Most cases are sporadic, but familial cases have been described, with some families including multiple affected members (Wamoscher and Farhi 1963). A previous study showed that the incidence of LCPD in first-degree relatives of index cases was 2.5%, which was 35 times higher than that in the general population (Hall 1986). These reports imply the presence of genes that control LCPD susceptibility. The common occurrence of LCPD-like hip changes in a few hereditary skeletal dysplasias, such as trichorhinophalangeal syndrome (OMIM 190350; Noltorp et al. 1986), also implies the presence of major causal genes for LCPD.

We recently encountered a family with an autosomal dominant hip disorder that co-segregated with a *COL2A1* mutation. *COL2A1* (OMIM 120140) encodes the α1(II) chain of type II collagen, which is a major structural protein in cartilage. In this family, some affected individuals presented with typical LCPD and cyclic changes, while others had very mild involvement and weak regeneration. This observation raised the hypothesis that derangement and/or modification of type II collagen plays a critical role in the etiology of LCPD. This is the first report of a mutation in hereditary LCPD.

Subjects and methods

Clinical report

A 13-year-old girl (III-4, Fig. 1) came to us with a painful limp and restricted motion of the right hip joint starting at 12 years of age. She had suffered from the precedent left hip pain. Her body height was 150 cm (−0.6 SD), and her body weight was 45 kg (−0.2 SD). A hip radiograph revealed small capital femoral epiphyses of both hip joints (Fig. 2a). Magnetic resonance imaging (MRI) showed subchondral signal alteration in the antero-lateral aspect of the bilateral capital femoral epiphyses with right predominance, implying osteonecrotic change (Fig. 2b). After five months of non weight-bearing activity, a follow-up MRI revealed a decreased epiphyseal signal. At 17 years of age, her left hip pain again increased. MRI analysis again showed increased signal alteration in the left hip joint. A skeletal survey including radiographs of the skull, spine, hands and lower extremities revealed no remarkable abnormalities aside from hypoplasia of the proximal femoral epiphyses (not shown). She was diagnosed as having mild LCPD.

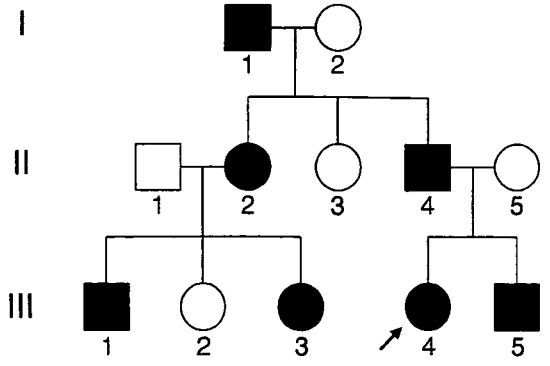

Fig. 1 Pedigree of the family of Legg-Calvé-Perthes disease. The *arrow* indicates the proband

The younger brother of the proband (III-5) was brought to medical attention with painful hip joints of several months' duration at 13 years of age. His height was 165.5 cm (0.4 SD), and his weight was 50 kg (−0.3 SD). A hip radiograph (Fig. 2c) showed mild flattening of the bilateral capital femoral epiphyses, and MRI revealed their subchondral signal changes. A skeletal survey showed only bipartite patella of the right knee and a Schmorl node in the endplate of the first lumbar spine. His symptoms had been relieved with rest. He was also diagnosed as having mild LCPD.

The sib affliction with this hip disorder prompted us to perform a pedigree analysis, which revealed an autosomal dominant mode of inheritance (Fig. 1). Two patients (I-1 and II-2) had undergone bilateral total hip arthroplasties at ages 60 and 42 years, respectively. The father of the proband (II-4) had suffered right hip pain at 5 years and 6 months of age. A radiograph of hip joints at age 7 years revealed flattening and fragmentation of the right capital femoral epiphysis (Fig. 3a), and he was diagnosed as having LCPD. At age 9 years, the left capital femoral epiphysis also was involved (Fig. 3b). The hip changes evolved from coxa plana with fragmentation, through the regeneration phase (Fig. 3c) to coxa magna with fair joint congruency typically seen as late sequelae of LCPD (Fig. 3d). A cousin of the proband (III-1) had right hip pain and was diagnosed as having LCPD at age 12. A hip radiograph showed collapse and fragmentation of the right capital femoral epiphysis, typical of LCPD (Fig. 2d). Another cousin (III-3) was asymptomatic but had hypoplastic capital femoral epiphyses similar to that of the proband (not shown). None of the affected members showed vitroretinal degeneration or hearing impairment, and none had any complicating factor including the use of steroid medications, alcohol consumption or systemic lupus erythematosus. Clinical findings for affected family members are summarized in Table 1.

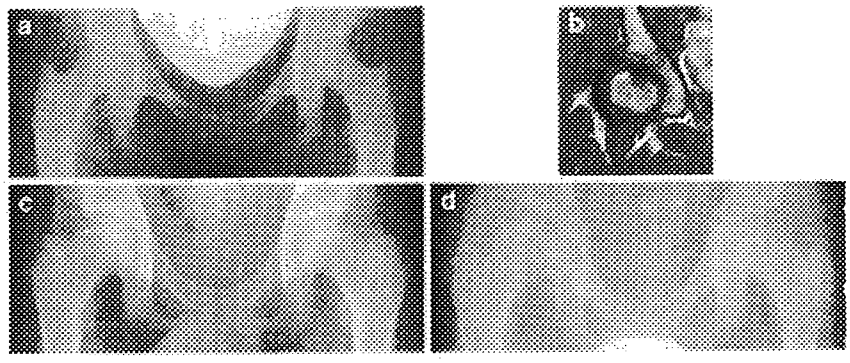

Fig. 2 Hip joints of patients. **a** Radiograph of the proband (III-4) at age 12. **b** T1-weighted MRI image of the left hip of the proband at the same age. **c** Radiograph of subject III-5 at age 13. **d** Radiograph of subject III-1 at age 12

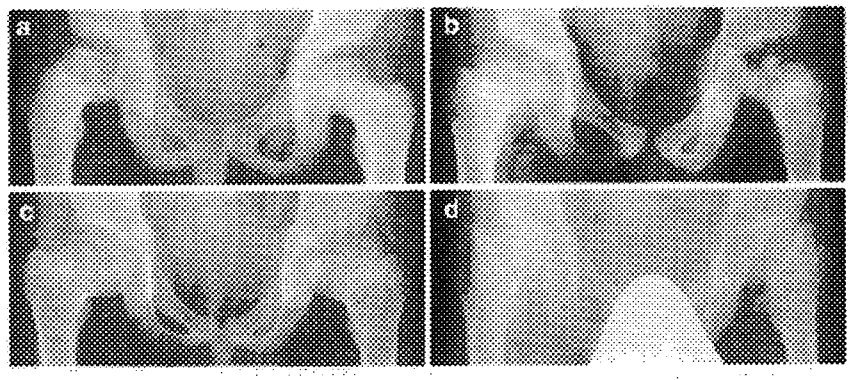

Fig. 3 Clinical course of hip joints of subject II-4 presenting with the typical LCPD. **a** At age 7, the right epiphysis has collapsed and fragmented; the left epiphysis is almost normal. **b** At age 9, the left epiphysis also has collapsed. **c** At age 11, both epiphyses are in a regeneration phase. **d** At age 45, note residual deformities of the femoral heads

Table 1 Summary of clinical findings of the affected members

Subject	Age (year)	Sex	Age at diagnosis (year)	Height (cm) (SD)	Diagnosis	Spinal changes
I-1	81	M	NA	165 (+1.0)	NA (Bilateral THA)	NA
II-2	49	F	15	160 (+0.3)	LCPD	–
II-4	45	M	5	167 (−0.7)	LCPD	–
III-1	20	M	12	168 (−0.5)	LCPD	Schmorl node
III-3	16	F	–	162 (+0.7)	Small femoral heads	–
III-4	20	F	13	151 (−1.2)	Mild LCPD	–
III-5	16	M	13	168 (−0.5)	Mild LCPD	Schmorl node

NA data not available or assessed, THA: total hip arthroplasty

Mutation analysis

Peripheral blood was obtained with informed consent from the family and control individuals. Ten members of the family were available for genetic analyses. Genomic DNA was extracted from blood using a standard method. Preliminary linkage analysis of the candidate genes was performed using ABI PRISM linkage mapping set Version 2.5 and an ABI Prism 3700 automated sequencer (Applied Biosystems, Foster, CA). The entire coding regions of *COL2A1* (GenBank accession number: NM_001844.3) with flanking intronic regions were examined by PCR and direct sequence analysis (Nishimura et al. 2005). Exon 50 and its flanking regions were amplified using primers *COL2A1*ex50SF (5′- tgagcatgt gaagaactggg-3′) and *COL2A1*ex50SR (5′- gacagcagggaagg agtcag-3′). PCR products were sequenced directly using an ABI Prism 3700 automated sequencer. PCR product including exon 50 was also analyzed by digestion with *Hpy*99I (New England Biolabs, Ipswich, MA).

Results

First, we examined the linkage between the phenotype and micro-satellite markers flanking candidate genes that could be responsible for dysplasia of capital femoral epiphyses, including *COL2A1*, *COL9A1-A3* (OMIMs 120210, 120260 and 120270, respectively), *MATN3* (OMIM 602109), *COMP* (OMIM 600310) and *DTDST* (OMIM 606718). Flanking markers for *COL2A1* (*D12S85* and *D12S368*) showed no recombination with the phenotype, while other genes were excluded (data not shown).

Next, we examined the entire coding regions of *COL2A1* with flanking intronic regions using PCR and direct sequencing. We identified a heterozygous c.3508G>A (the A of the first ATG is denoted as +1) mutation within exon 50 (Fig. 4a). The mutation was not found in 80 unrelated Japanese control individuals, and no other mutations were found in the analyzed region. Co-segregation of the mutation with the phenotype was examined by PCR-RFLP

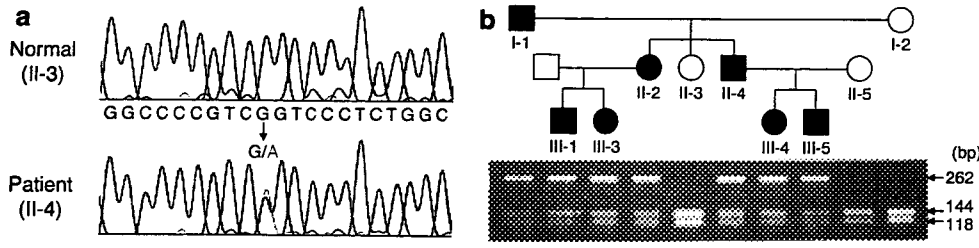

Fig. 4 A *COL2A1* mutation in the family (c.3508G>A; the A of the first ATG is denoted as +1). **a** Genomic sequences around the mutation of unaffected (II-3) and affected (II-4) members. **b** Co-segregation of the *COL2A1* mutation. PCR products including exon 50 of *COL2A1* were digested with *Hpy*99I. The amplicon with the normal allele yielded 144-bp and 118-bp fragments; the amplicon with the mutant allele yielded a 262-bp fragment

analysis using *Hpy*99I. All affected members had the heterozygous mutation, whereas all unaffected members did not (Fig. 4b). This co-segregation was confirmed by direct sequencing.

Discussion

We have identified a *COL2A1* mutation in a large Japanese family with an inherited hip disorder that manifests as LCPD. This is the first report of a mutation linked to hereditary LCPD. The mutation (p.G1170S) leads to an amino acid change that perturbs a Gly-X-Y triple-helix repeat, which is a fundamental structure in type II collagen. The presence of abnormal large-diameter collagen fibrils in the epiphyseal cartilage of LCPD patients has been reported (Ponseti et al. 1983). This implies that abnormal type II collagen could be the cause of LCPD. Furthermore, stress fracture of the femoral head was suggested to be important in the development of LCPD (Caffey 1968). It is tempting to assume that weak joint cartilage and abnormal subchondral trabeculae as a result of *COL2A1* mutations are vulnerable to subchondral stress fracture of the femoral head, resulting in LCPD.

COL2A1 mutations, or type II collagenopathies, cause several types of skeletal dysplasias that primarily affect capital femoral epiphyses in growing children, such as spondyloepiphyseal dysplasia congenita (OMIM 183900), Kniest dysplasia (OMIM 156550), Stickler dysplasia (OMIM 108300), oto-spondylo-megaepiphyseal dysplasia (OMIM 215150; Miyamoto et al. 2005) and spondyloepiphyseal dysplasia with premature onset arthrosis (OMIM 208230). The epiphyseal dysplasias in these disorders are basically congenital, symmetrical and progressive. Typically, they do not show the regeneration phase seen in LCPD and in the family described here. Patients in this family had normal stature and no ocular or hearing impairment. These findings, as well as the lack of spinal dysplasia, are atypical for type II collagenopathies (Nishimura et al. 2005). *COL2A1* mutations also cause precocious osteoarthritis (Williams et al. 1993). However, the condition is characterized by progressive joint space narrowing, and, unlike LCPD, does not show a regeneration phase.

In spite of harboring the same mutation, the phenotypes of affected family members varied considerably in course and severity. Patients II-4 and III-1 followed the typical clinical courses of LCPD with cyclic changes. Patients III-4 and III-5 had a milder form, which was described as group 1 by Catterall (1971). The phenotypes of III-4 and III-5 might also be described as early-onset ANFH, although both patients have yet to reach skeletal maturity. Recently, Liu et al. (2005) reported two *COL2A1* mutations in Taiwanese families with adult-onset ANFH. The mutation identified in our study is the same as that reported in these two families, wherein affected members had adult-onset idiopathic ANFH with an average age at onset of 26 years (Chen et al. 2004). No affected individual in the Taiwanese families showed evidence of LCPD. These intra- and interfamilial variations in patients' clinical and radiographic courses of patients harboring identical mutations suggest that environmental factors or other genetic factors may affect patients' outcome.

Osteonecrosis is common to both LCPD and ANFH, but these disorders differ in both age of onset and clinical course. In LCPD, affected capital femoral epiphyses regenerate to a certain degree, but in ANFH they do not. The time remaining before closure of the capital femoral growth plate is thought to be important in determining the prognosis of LCPD (Mazda et al. 1999). We speculate that in both LCPD and ANFH, osteonecrosis may arise via the same mechanism in which abnormal type II collagen engages. Thus, osteonecrosis would precipitate LCPD phenotypes if it occurs prior to closure of the growth plate and ANFH phenotypes if it occurs following closure.

Through this study we have extended the phenotypic spectrum of *COL2A1* mutations. Such mutations may be more common in LCPD patients than currently thought, particularly in familial and/or bilateral cases. If so, examination of the *COL2A1* mutation could have great impact on diagnosis and treatment of LCPD, by enabling more accurate prediction of the risk and the prognosis. A large-scale screen for *COL2A1* mutations in LCPD patients should be considered.

Acknowledgements We thank the patients and their family for their cooperation, Dr. Hidekazu Touga for supporting the research, Dr. Kazuharu Takikawa for valuable advice and critical reading of the manuscript and Yoshie Takanashi for the excellent technical assistance. This work was supported by Grants-in-aid from Research on Child Health and Development from Ministry of Health, Labor and Welfare of Japan (Contract grant number: 17C-1, H18-005) and from Ministry of Education, Culture, Sports and Science of Japan (Contract grant number: 18390423).

References

Caffey J (1968) The early roentgenographic changes in essential coxa plana: their significance in pathogenesis. Am J Roentgenol Radium Ther Nucl Med 103:620–634

Catterall A (1971) The natural history of Perthes' disease. J Bone Joint Surg Br 53:37–53

Chen WM, Liu YF, Lin MW, Chen IC, Lin PY, Lin GL, Jou YS, Lin YT, Fann CS, Wu JY, Hsiao KJ, Tsai SF (2004) Autosomal dominant avascular necrosis of femoral head in two Taiwanese pedigrees and linkage to chromosome 12q13. Am J Hum Genet 75:310–317

Dilley A, Hooper WC, Austin H, Jamil M, Miller C, Stokes M, Evatt B, Eldridge J (2003) The beta fibrinogen gene G-455-A polymorphism is a risk factor for Legg-Perthes disease. J Thromb Haemost 1:2317–2321

Glueck CJ, Crawford A, Roy D, Freiberg R, Glueck H, Stroop D (1996) Association of antithrombotic factor deficiencies and hypofibrinolysis with Legg-Perthes disease. J Bone Joint Surg Am 78:3–13

Glueck CJ, Freiberg RA, Crawford A, Gruppo R, Roy D, Tracy T, Sieve-Smith L, Wang P (1998) Secondhand smoke, hypofibrinolysis, and Legg-Perthes disease. Clin Orthop Relat Res 352:159–167

Gruppo R, Glueck CJ, Wall E, Roy D, Wang P (1998) Legg-Perthes disease in three siblings, two heterozygous and one homozygous for the factor V Leiden mutation. J Pediatr 132:885–888

Hall DJ (1986) Genetic aspects of Perthes' disease. A critical review. Clin Orthop Relat Res 209:100–114

Liu YF, Chen WM, Lin YF, Yang RC, Lin MW, Li LH, Chang YH, Jou YS, Lin PY, Su JS, Huang SF, Hsiao KJ, Fann CS, Hwang HW, Chen YT, Tsai SF (2005) Type II collagen gene variants and inherited osteonecrosis of the femoral head. N Engl J Med 352:2294–2301

Mackenzie WG, Bassett GS, Mandell GA, Scott CI Jr (1989) Avascular necrosis of the hip in multiple epiphyseal dysplasia. J Pediatr Orthop 9:666–671

Margetts BM, Perry CA, Taylor JF, Dangerfield PH (2001) The incidence and distribution of Legg-Calve-Perthes' disease in Liverpool, 1982–1995. Arch Dis Child 84:351–354

Mazda K, Pennecot GF, Zeller R, Taussig G (1999) Perthes' disease after the age of twelve years. Role of the remaining growth. J Bone Joint Surg Br 81:696–698

Miyamoto Y, Nakashima E, Hiraoka H, Ohashi H, Ikegawa S (2005) A type II collagen mutation also results in oto-spondylo-megaepiphyseal dysplasia. Hum Genet 118:175–178

Nishimura G, Haga N, Kitoh H, Tanaka Y, Sonoda T, Kitamura M, Shirahama S, Itoh T, Nakashima E, Ohashi H, Ikegawa S (2005) The phenotypic spectrum of COL2A1 mutations. Hum Mutat 26:36–43

Noltorp S, Kristoffersson UL, Mandahl N, Stigsson L, Svensson B, Werner CO (1986) Trichorhinophalangeal syndrome type I: symptoms and signs, radiology and genetics. Ann Rheum Dis 45:31–36

Pillai A, Atiya S, Costigan PS (2005) The incidence of Perthes' disease in Southwest Scotland. J Bone Joint Surg Br 87:1531–1535

Ponseti IV, Maynard JA, Weinstein SL, Ippolito EG, Pous JG (1983) Legg-Calve-Perthes disease. Histochemical and ultrastructural observations of the epiphyseal cartilage and physis. J Bone Joint Surg Am 65:797–807

Rowe SM, Jung ST, Lee KB, Bae BH, Cheon SY, Kang KD (2005) The incidence of Perthes' disease in Korea: a focus on differences among races. J Bone Joint Surg Br 87:1666–1668

Thompson GH, Price CT, Roy D, Meehan PL, Richards BS (2002) Legg-Calve-Perthes disease: current concepts. Instr Course Lect 51:367–384

Wamoscher Z, Farhi A (1963) Hereditary Legg-Calve-Perthes disease. Am J Dis Child 106:97–100

Williams CJ, Considine EL, Knowlton RG, Reginato A, Neumann G, Harrison D, Buxton P, Jimenez S, Prockop DJ (1993) Spondyloepiphyseal dysplasia and precocious osteoarthritis in a family with an Arg75–>Cys mutation in the procollagen type II gene (COL2A1). Hum Genet 92:499–505

American Journal of Medical Genetics Part A 143A:884–887 (2007)

Clinical Report

Spinal Extradural Arachnoid Cysts Associated With Distichiasis and Lymphedema

Shoji Yabuki,[1]* Shin-ichi Kikuchi,[1] and Shiro Ikegawa[2]

[1]Department of Orthopaedic Surgery, Fukushima Medical University School of Medicine, Fukushima, Japan
[2]Laboratory for Bone and Joint Diseases, SNP Research Center, RIKEN, Tokyo, Japan

Received 26 June 2006; Accepted 29 November 2006

Spinal extradural arachnoid cysts (SEDAC) are lesions communicating to the subarachnoid space of the spinal canal via a dural defect. SEDAC occupies intraspinal space and sometimes causes neurological disturbances. Although most reported cases are sporadic, several familial cases have been described, suggesting a genetic etiology. Here we report on a family with SEDAC inherited in an autosomal dominant mode. Detailed study showed that the family has the lymphedema-distichiasis syndrome. Among family members examined, a total of ten in two generations manifested all or some of the following features: SEDAC, distichiasis and lymphedema. Seven had spinal cysts, four had both SEDAC and distichiasis, and one had SEDAC distichiasis and lymphedema; three did not have SEDAC. These findings, together with rarity of both distichiasis and lymphedema in the general population, support that all of the ten members were affected with one clinical entity, the lymphedema-distichiasis syndrome. The distribution of features illustrates the variable expressivity of clinical manifestations. Although *FOXC2* mutation analysis was not performed in our family, it is likely that SEDAC is a component manifestation of lymphedema-distichiasis syndrome and more consistent in our family than those reported.

Key words: spinal extradural cyst; familial case; lymphedema-distichiasis syndrome

How to cite this article: Yabuki S, Kikuchi S, Ikegawa S. 2007. Spinal extradural arachnoid cysts associated with distichiasis and lymphedema. Am J Med Genet Part A 143A:884–887.

INTRODUCTION

Spinal extradural arachnoid cyst (SEDAC), a relatively rare condition, communicates to the subarachnoid space of the spinal canal via a dural defect. These lesions occupy the intraspinal space and sometimes cause neurological disturbances such as compression myelopathy [McCrum and Williams, 1982; Prevo et al., 1999; Chang et al., 2004; Novak et al., 2005]. Although SEDAC represents 1% of all primary spinal cord tumors [Elsberg et al. 1934], the number of reported cases has recently increased with the more widespread use of MRI [Takagaki et al., 2006]. Nevertheless, its etiology and pathogenesis has remained undetermined. Hypotheses proposed include: the occurrence (1) secondary to previous surgery such as laminectomy, discectomy or lumbar puncture, (2) by arachnoid proliferation, (3) by congenital dural defect or weakness, and (4) by closed spinal trauma [Miravet et al., 2002]. Most reported cases are sporadic, but familial cases have been described [Chynn, 1967; Bergland, 1968; Robinow et al., 1970; Schwartz et al., 1980]. Chynn [1967] first reported a pair of siblings with SEDAC and suggested a role of genetic etiology. Bergland [1968] reported a more extensive pedigree of the same family, which also showed associated occurrence of distichiasis (extra rows of eyelashes) and Milroy disease (lymphedema of lower extremities). Robinow et al. [1970] reported familial SEDAC coexisting with distichiasis and lymphedema of the lower extremities. These families suggested that SEDAC

Grant sponsor: Fukushima Society for the Promotion of Medicine; Grant sponsor: Scientific Research from Child Health and Development; Grant number: 17C-1; Grant sponsor: Ministry of Education, Culture, Sports and Science of Japan; Grant number: 183904230; Grant sponsor: Research on Children and Families from the Ministry of Health, Labor and Welfare; Grant number: H18-005.

*Correspondence to: Shoji Yabuki, M.D., Department of Orthopaedic Surgery, Fukushima Medical University School of Medicine, 1 Hikarigaoka, Fukushima, Fukushima 960-1295, Japan.
E-mail: yabuki@fmu.ac.jp

Published online 15 March 2007 in Wiley InterScience (www.interscience.wiley.com)
DOI 10.1002/ajmg.a.31669

is causally related to lymphedema-distichiasis syndrome, that is, an autosomal dominant disorder (OMIM #153400).

Here we report on a family where 10 members were affected with all or either of SEDAC, distichiasis and lymphedema of lower extremities. Of the 10 affected members, four manifested both SEDAC and distichiasis, two distichiasis and lymphedema, and three did not have SEDAC.

CLINICAL REPORTS

The proband (III-5, Fig. 1) was a 12-year-old girl who presented with gait disturbance and motor weakness of the lower extremities caused by spinal cord compression. Her height was 155 cm (+0.5 SD) and weight 53 kg (+1.0 SD). She demonstrated hyper-reflexia in her lower extremities and positive sign of the Babinski reflex bilaterally. MRI scan showed multiple extradural arachnoid cysts in her thoracic spine (Fig. 2).

Family history revealed that there was no consanguineous marriage, but a cousin (III-1) 2 years older than the proband also had received surgery for SEDAC. This suggested that the condition is familial. We examined other family members for spinal cysts. MRI of the thoracic and lumbar spine were obtained from family members with informed consent. A 4-year-old girl (III-9) was excluded from the study because she was too young to provide consent. The study protocol was approved by the institutional ethical committee.

T1 and T2 weighted images in the sagittal plane were evaluated for the presence or absence of SEDAC by one (S.Y.) of us. In total, seven family members were found to have SEDAC (Fig. 1, Table I), and four had multiple cysts. A mode of inheritance for the disease was autosomal dominant with variable expression. No family members had signs suggestive of Marfan syndrome, neurofibromatosis or lateral meningocele syndrome [Lehman et al., 1977; Gripp et al., 1997]. Clinical examinations revealed that, in addition to the seven individuals with spinal cysts, three members (II-1, II-3, and III-3) had either or both of distichiasis and lymphedema of lower extremities, regardless of SEDAC. Of a total of 10 affected members, seven manifested distichiasis (two were not examined). Two of them (II-1 and II-6) had both distichiasis and lymphedema of lower extremities, and three (II-1, II-3 and III-3) did not have SEDAC (Fig. 1, Table I).

Three of the seven SEDAC patients had symptoms caused by spinal cord compression that necessitated surgery (Table I). Their symptoms included gait disturbance and motor weakness of lower extremities (III-1 and III-5) and back pain (III-2). Neurological examination showed hyper-reflexia of the patella tendon reflex and the Achilles tendon reflex in all the three individuals. Hypesthesia of lower extremities was seen in individuals III-1 and III-5. These individuals showed the following similar operative findings: SEDAC detected after opening the laminae; and the cysts communicating to the subarachnoid space via a stalk (dural defect) that existed at the postero-lateral aspect of the dura mater just cranial to a nerve root and was closed using a vascular clip. All the three patients recovered completely after the surgery.

DISCUSSION

We have reported on a family in which seven of 10 members with the lymphedema distichiasis syndrome have SEDAC. The high occurrence of SEDAC is notable but we have investigated our family for SEDAC in a comprehensive manner.

SEDAC may share similar pathogenesis with dural ectasia, a widening of the dura mater, because both conditions show similar morphological changes in the dural sac [O'Neill et al., 1983]. It has been

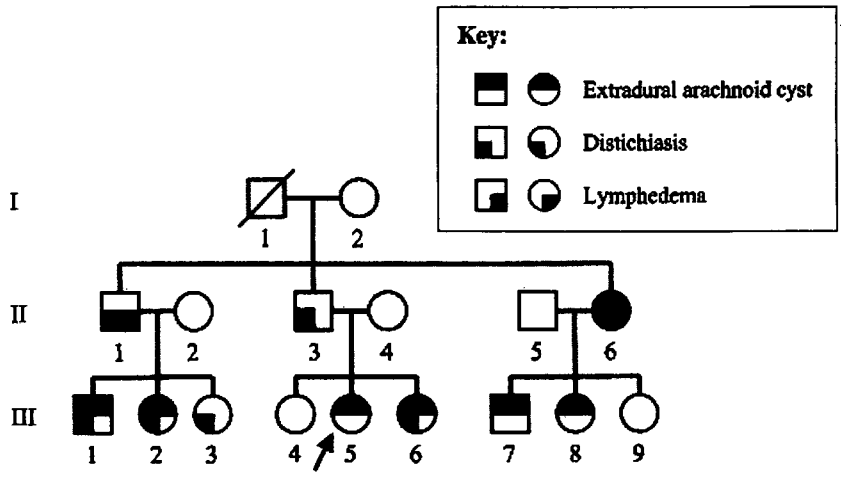

FIG. 1. Pedigree of a Japanese family with spinal extradural arachnoid cyst. Individuals II-2 and III-9 did not receive MRI examination.

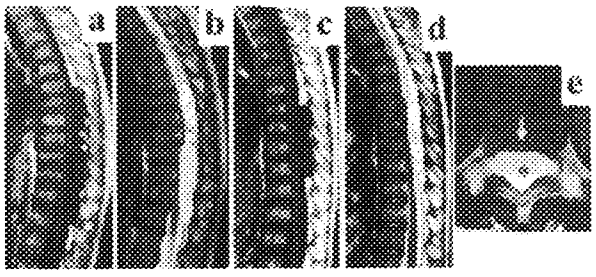

FIG. 2. MRI of family members with spinal extradural arachnoid cysts. Sagittal planes of the thoracolumbar spine (**a–d**) showing multiple cysts dorsal to the spinal cord in the proband (III-5, a and b) and in III-2 (c and d). a and c: T1 weighted image; **b** and **d**: T2 weighted image. Axial plane (T2 weighted image) at T10/11 disc level in III-5 (**e**) showing expanding of the cyst within the spinal canal. Arrow and asterisk depict spinal cord and extradural arachnoid cyst, respectively.

speculated that dural ectasia arises from continuous, somewhat pulsatile pressure of cerebrospinal fluid on a connective-tissue membrane that is weakened by a defect in the extracellular matrix [Pyeritz et al., 1988]. Dural ectasia is seen in some heritable connective tissue disorders, such as NF types 1 and 2 [O'Neill et al., 1983; Jamjoom et al., 1990; Eichhorn et al., 1995], Marfan syndrome (MS) types 1 and 2 [Pyeritz et al., 1988; Stern, 1988], and lateral meningocele syndrome (LMS) [Lehman et al., 1977; Gripp et al., 1997]. The extent of their extradural arachnoid cysts was limited to the spinal canal (Fig. 2E), the findings being different from dural ectasia seen in NF, MS, and LMS.

Distichiasis and lymphedema of lower extremities are sometimes associated with SEDAC. One of two patients reported by Chynn [1967] had distichiasis, a history of bronchial asthma and familial lymphedema of their right lower extremity (Milroy disease), while the other manifested only distichiasis. All three patients reported by Bergland [1968] had distichiasis, and one had Milroy disease. Two of three patients by Robinow et al. [1970] had both distichiasis and lymphedema of the lower extremities, and the other manifested only distichiasis. In an autosomal dominant condition reported by Falls and Kertesz [1964], abnormal lymphatics of the lower extremities are associated with pterygium colli and eyelid anomalies, but incidence of SEDAC was not specified. Schwartz et al. [1980] reported two adolescent sibs and their mother with spinal arachnoid cyst at an intradural sac, double rows of eyelashes and lymphedema of lower extremities. In the family we have reported, of a total of 10 affected members, seven had SEDAC, seven manifested distichiasis with or without SEDAC, and three had only lymphedema and/or distichiasis. There was only one individual who manifested all. These findings, together with rarity of both double-eyelashes and lymphedema in the general population, support that all of the ten members in our family were affected with one clinical entity, that is, lymphedema-distichiasis syndrome, which shows the variable expressivity of clinical manifestations. It has been reported that protein-truncating mutations in *FOXC2*, the forkhead family transcription factor gene, cause lymphedema-distichiasis syndrome. The syndrome is associated with variable abnormalities, such as cardiac defects, cleft palate, and photophobia [Fang et al., 2000; Erickson et al., 2001; Finegold et al., 2001; Sholto-Douglas-Vernon et al., 2005]. Although *FOXC2* mutation analysis was

TABLE I. Clinical Data of Members in the Present Family

Individuals	Age (years)	Sex	SEADC +/−	SEADC Number	SEADC Site	SEADC Surgery	Distichiasis	Lymphedema of lower extremity	vRNF	MS	LM
I-2	65	F	−	−	−	−	−	−	−	−	−
II-1	35	M	−	−	−	−	+	+	−	−	−
II-2	33	F	n.s.	n.s.	n.s.	−	−	−	−	−	n.s.
II-3	40	M	−	−	−	−	+	−	−	−	−
II-4	39	F	−	−	−	−	−	−	−	−	−
II-5	37	M	−	−	−	−	n.s.	n.s.	n.s.	n.s.	−
II-6	38	F	+	Single	T9	−	+	+	−	−	−
III-1	15	M	+	Multiple	T11-S1	+	+	−	−	−	−
III-2	13	F	+	Multiple	T5-T10, L4-L5	+	+	−	−	−	−
III-3	10	F	−	−	−	−	+	−	−	−	−
III-4	14	F	−	−	−	−	n.s.	n.s.	n.s.	n.s.	−
III-5	12	F	+	Multiple	T5-T12	+	−	−	−	−	−
III-6	7	F	+	Multiple	T7-T10, L4-S2	−	+	−	−	−	−
III-7	10	M	+	Single	T8-T9	−	n.s.	n.s.	n.s.	n.s.	−
III-8	7	F	+	Single	T2-T5	−	n.s.	n.s.	n.s.	n.s.	−
III-9	4	F	n.s.	n.s.	n.s.	−	n.s.	n.s.	n.s.	n.s.	n.s.

SEDAC, spinal extradural arachnoid cyst; +/−, presence or absence; vRNF, von Recklinghausen neurofibromatosis; MS, Marfan syndrome; LM, lateral meningocele; F, female; M, male; n.s., not studied.

not done in our family, it is likely that SEDAC is a component manifestation of lymphedema-distichiasis syndrome. It remains to be seen what the actual frequency of SEDAC is in lymphedema-distichiasis syndrome have SEDAC.

ACKNOWLEDGMENTS

We express our gratitude to members of the family for participating in this study. Research grant from the Fukushima Society for the Promotion of Medicine for S.Y., and Grants-in-aid for Scientific Research from Child Health and Development (No. 17C-1), Research on Children and Families from the Ministry of Health, Labor and Welfare (H18-005) and from Ministry of Education, Culture, Sports and Science of Japan (No. 183904230) for S.I.

REFERENCES

Bergland RM. 1968. Congenital intraspinal extradural cyst: Report of three cases in one family. J Neurosurg 28:495–499.

Chang IC, Chou MC, Bell WR, Lin ZI. 2004. Spinal cord compression caused by extradural arachnoid cysts. Pediatr Neurosurg 40:70–74.

Chynn KY. 1967. Congenital spinal extradural cyst in two siblings. Am J Roentgenol 101:204–215.

Eichhorn C, Wendt G, Staudte HW, Gilsbach JM. 1995. Dural ectasia in von Recklinghausen's disease of the lumbar spine: A case report. J Bone Joint Surg 77B:834–835.

Elsberg CA, Dyke CG, Brewer ED. 1934. The symptoms and diagnosis of extradural cysts. Bull Neurol Inst NY 3:395–417.

Erickson RP, Dagenais SL, Caulder MS, Downs CA, Herman G, Jones MC, Kerstjens-Frederikse WS, Lindral AC, McDonald M, Nelson CC, Witte M, Glover TW. 2001. Clinical heterogeneity in lymphoedema-distichiasis with *FOXC2* truncating mutations. J Med Genet 38:761–766.

Falls HF, Kertesz ED. 1964. A new syndrome combining pterygium colli with developmental anomalies of the eyelids and lymphatics of the lower extremities. Tr Am Ophth Soc 62:248–275.

Fang J, Dagenais SL, Erickson RP, Arlt MF, Glynn MW, Gorski JL, Seaver LH, Glover TW. 2000. Mutations in *FOXC2 (MFH-1)*, a forkhead family transcription factor, are responsible for hereditary lymphedema-distichiasis syndrome. Am J Hum Genet 67:1382–1388.

Finegold DN, Kimak MA, Lawrence EC, Levinson KL, Cherniske EM, Porter BR, Dunlap JW, Ferrell RE. 2001. Truncating mutations in *FAXC2* cause multiple lymphedema syndromes. Hum Mol Genet 10:1185–1189.

Gripp KW, Scott CI Jr, Hughes HE, Wallerstein R, Nicholson L, States L, Bason LD, Kaplan P, Zderic SA, Duhaime AC, Miller F, Magnusson MR, Zackai EH. 1997. Lateral meningocele syndrome: Three new patients and review of the literature. Am J Med Genet 70:229–239.

Jamjoom ZAB, Malabarey T, Kolawole TM, Araby K. 1990. Lumbosacral dural anomalies in von Recklinghausen neurofibromatosis. Acta Neurochir (Wien) 105:140–146.

Lehman RA, Stears JC, Wesenberg RI, Nusbaum ED. 1977. Familial osteosclerosis with abnormalities of the nervous system and menings. J Pediatr 90:49–54.

McCrum C, Williams B. 1982. Spinal extradural arachnoid pouches: Report of two cases. J Neurosurg 57:849–852.

Miravet E, Sinisterra S, Birchansky S, Papazian O, Tuite G, Grossman JAL, Alfonso I. 2002. Cervicothoracic extradural arachnoid cyst: Possible association with obstetric brachial plexus pulsy. J Child Neurol 17:770–772.

Novak L, Dobai J, Nemeth T, Fekete M, Prinzinger A, Csecsei GI. 2005. Spinal extradural arachnoid cysts causing cord compression in a 15-year-old girl: A case report. Zentralbl Neurochir 66:43–46.

O'Neill P, Whatmore WJ, Booth AE. 1983. Spinal meningocele in association with neurofibromatosis. Neurosurgery 13:82–84.

Prevo RL, Hageman G, Bruyn RPM, Broere G, van de Stadt J. 1999. Extended extradural spinal arachnoid cyst: An unusual cause of progressive spastic paraparesis. Clin Neurol Neurosurg 101:260–263.

Pyeritz RE, Fishman EK, Bernhardt BA, Siegelman SS. 1988. Dural ectasia is a common feature of the Marfan syndrome. Am J Hum Genet 43:726–732.

Robinow M, Johnson GF, Verhagen AD. 1970. Distichiasis-lymphedema: A hereditary syndrome of multiple congenital defects. Am J Dis Child 119:343–347.

Schwartz JF, O'Brien MS, Hoffman JC Jr. 1980. Hereditary spinal arachnoid cysts, distichialis, and lymphedema. Ann Neurol 7:340–343.

Sholto-Douglas-Vernon C, Bell R, Brice G, Mansour S, Sarfarazi M, Child AH, Smith A, Mellor R, Burnand K, Mortimer P, Jeffery S. 2005. Lymphoedema-distichiasis and *FOX C2*: Unreported mutations, de novo mutation estimate, families without coding mutations. Hum Genet 117:238–242.

Stern WE. 1988. Dural ectasia and the Marfan syndrome. J Neurosurg 69:221–227.

Takagaki T, Nomura T, Toh E, Watanabe M, Mochida J. 2006. Multiple extradural arachnoid cyst at the spinal cord and cauda equina levels in the young. Spinal Cord 44:59–62.

American Journal of Medical Genetics Part A 143A:1703–1707 (2007)

GPC3 Mutations in Seven Patients With Simpson–Golabi–Behmel Syndrome

Satoru Sakazume,[1,6,7]* Nobuhiko Okamoto,[2] Toshiyuki Yamamoto,[3,4] Kenji Kurosawa,[4] Hironao Numabe,[5] Yuko Ohashi,[1] Yuko Kako,[1] Toshiro Nagai,[6,8] and Hirohumi Ohashi[1]

[1]Division of Medical Genetics, Saitama Children's Medical Center, Saitama, Japan
[2]Department of Planning and Research, Osaka Medical Center and Research Institute for Maternal and Patient Health, Osaka, Japan
[3]International Research and Educational Institute for Integrated Medical Sciences, Tokyo Women's Medical University, Tokyo, Japan
[4]Division of Medical Genetics, Kanagawa Children's Medical Center, Yokohama, Japan
[5]Department of Medical Genetics, Kyoto University Hospital, Kyoto, Japan
[6]Department of Pediatrics, Koshigaya Hospital, Dokkyo University School of Medicine, Koshigaya, Japan
[7]Division of Medical Genetics, Gunma Children's Medical Center, Shibukawa, Gunma, Japan
[8]Solution Oriented Research for Science and Technology (SORST), Japan Science and Technology (JST), Kawaguchi, Japan

Received 13 September 2006; Accepted 19 March 2007

We analyzed mutations of the *GPC3*gene in seven males with typical manifestations of Simpson–Golabi–Behmel syndrome (SGBS). Genomic DNA was PCR amplified for its all eight exons and exon–intron boundaries using designed set of primers, and PCR products were directly sequenced. All eight males studied had mutations: One patient had a large deletion spanning introns 6 and 7, four each had a C → T base substitution resulting in a stop codon formation in exons 2, 3, and 4, one had a single-base insertion in exon 2, and the other had a six-base deletion and a three-base insertion in exon 3; all resulting in loss-of-function of the glypican-3 protein. These results, together with previous studies of *GPC3* mutations, indicate that there is no hot spot for *GPC3* mutations or deletions in the patients with the syndrome. Also, no correlation has been noted between the location and nature of mutations and the phenotype of the patients studied, as is the case of the present study.

Key words: Simpson–Golabi–Behmel syndrome (SGBS); overgrowth syndrome; *GPC3* mutation

How to cite this article: Sakazume S, Okamoto N, Yamamoto T, Kurosawa K, Numabe H, Ohashi Y, Kako Y, Nagai T, Ohashi H. 2007. *GPC3* mutations in seven patients with Simpson–Golabi–Behmel syndrome. Am J Med Genet Part A 143A:1703–1707.

INTRODUCTION

Simpson–Golabi–Behmel syndrome (SGBS) is an X-linked MCA/MR syndrome characterized by pre- and postnatal overgrowth, "coarse" facial appearance, cleft lip and palate, macroglossia, a mild groove of the lower lip and/or tongue, supernumerary nipples, and various visceral and skeletal anomalies including congenital cardiac defects, diaphragmatic hernia, enlarged and dysplastic kidneys, and vertebral and rib anomalies [Neri et al., 1988]. The spectrum of its manifestations is broad, with phenotypes varying from very mild form to infantile lethal forms [Terespolsky et al., 1995]. The syndrome is also associated with a high risk for the development of embryonic tumors, including Wilms tumor and neuroblastoma during early childhood [Lapunzina, 2005]. Mutations in the *GPC3* gene at Xq26 were shown to cause SGBS in two female patients with X-autosome translocations [Pilia et al., 1996]. *GPC3* spans more than 500 kb of genomic DNA, contains eight exons, and encodes glypican-3 protein, i.e., a cell-surface heparan sulfate proteoglycan that plays a role in the control of cell growth and cell division by acting on Igf2 receptor in the presence of Igf2 [Pellegrini et al., 1998]. *GPC3* mutations so far

Grant sponsor: Ministry of Health, Labor, and Welfare of Japan; Grant sponsor: Kawano Masanori Memorial Foundation for Promotion of Pediatrics.
*Correspondence to: Dr. Satoru Sakazume, Division of Medical Genetics, Gunma Children's Medical Center, 779 Shimohakoda, Hokkitu, Shibukawa, Gunma 377-8577, Japan.
E-mail: saka377@gcmc.pref.gunma.jp
Published online 29 June 2007 in Wiley InterScience (www.interscience.wiley.com)
DOI 10.1002/ajmg.a.31822

reported in SGBS included large and small deletions, point mutations, and frameshift mutations, distributed throughout the entire gene without any mutational hot spots [Hughes-Benzie et al., 1996; Pilia et al., 1996; Lindsay et al., 1997; Veugelers et al., 1998; Okamoto et al., 1999; Xuan et al., 1999; Veugelers et al., 2000; Li et al., 2001; Mariani et al., 2003; Rodriguez-Criado et al., 2005]. While loss-of-function of glypican-3 is believed as the pathogenesis for SGBS, no genotype/phenotype correlation has yet been established.

Herein, we describe the results of *GPC3* mutation analysis in seven Japanese patients with typical SGBS.

MATERIALS AND METHODS

Patients

Seven male patients with SGBS, ranging in age from 15 months to 15 years (average 7 years), were ascertained by clinical geneticists (Table I, Fig. 1). Six patients were sporadic, whereas one (Patient 5) was familial having a younger brother with prenatal overgrowth, accessory nipples, and high-arched palate. G-banded chromosomes in the seven patients were all 46,XY.

Mutation Analysis of *GPC3*

We designed PCR primers capable of amplifying each of the eight exons and exon–intron junctions of *GPC3* with a single PCR reaction (Table II). In five of the seven patients, our newly designed primers were used with following protocol: Blood samples or lymphoblastoid cells were collected from the patients, and genomic DNA was extracted following standard methods; PCR reaction was performed using AmpliTaq Gold DNA polymerase (Applied Biosystems, Foster City, CA) with 10% DMSO in PCR buffer, and according to a touch-down PCR protocol [Sambrook and Russell, 2001]. Briefly, enzyme activation at 96°C for 5 min was followed by denaturation at 96°C for 30 sec, and extension at 72°C for 30 sec. First-cycle annealing was performed at 65°C for 30 sec. In the following 9 cycles, temperature was decreased from 65°C stepwise by one degree to 56°C, and maintained at 55°C throughout the remaining cycles. A total of 45 cycles were carried out with an ABI2400 thermal cycler. Amplification products were electrophoresed with TAE 1% agarose gel, and sequenced using an ABI310 sequencer and Big Dye Terminator ver3.1 cycle sequence kit (Applied Biosystems). In Patients 6 and 7, PCR had already been carried out (by one of us, T.Y.) using the primers of Huber et al. [1997] before designing the primers above. In Patient 7, amplification of exon 7 was unsuccessful. In view of this, a pair of intronic primers, each placed in introns 6 and 7, was used in the reaction (Table II).

RESULTS

Mutations or deletions causative of the syndrome were identified in all the seven patients studied (Table III). Four patients had C→T substitutions resulting in stop codon formation: Patients 1 and 2 in exon 3, Patient 3 in exon 4, and Patient 6 in exon 2. Patient 4 had a single-base insertion in exon 2, and thereby, frameshift change of codon 116 in exon 3, leading to a stop codon. Patient 5 showed a 6-bp deletion and 3-bp insertion in exon 3 causing a nonsense mutation. PCR of the genomic DNA from Patient 7 failed to amplify exon 7. PCR using primers placed in introns 6 and 7 resulted in abnormally

TABLE I. Clinical and Laboratory Findings in Seven Patients with Simpson–Golabi–Behmel Syndrome (SGBS)

	Patients							
	1	2	3	4	5	6	7	Total
Age (year)	3	10	9 months	8	15 months[a]	15	3	
Sex	Male	Male	Male	Male	Male	Male	Male	
Birth weight (SD)	+1.5	+0.8	+2.6	+2.6	+3.8	+2.6	+2.7	7/7
Postnatal overgrowth (height SD)		+1		+3.5		+3.5	+3.1	4/7
Delayed speech	+	+	+	+	−	+	−	5/7
Delayed motor milestones	+	+	+	+	+	+	−	6/7
CNS abnormalities	−	−	−	−	−	−	−	0
Characteristic facial features	+	+	+	+	+	+	+	7/7
Cleft lip and/or palate	CL&P	CL	CL	−	−	−	−	3/7
Macroglossia	+	+	+	+	+	+	+	7/7
Supernumerary nipples	+	−	−	−	+	+	+	4/7
Cardiac defects	−	−	−	−	−	−	−	0
Diaphragmatic hernia	+	−	−	−	+	−	−	2/7
Umbilical or inguinal hernia	+	−	−	−	−	+	−	2/7
Urinary tract abnormalities	+	−	−	−	−	−	+	2/7
Skeletal abnormalities	+	n	n	+	−	+	−	3/5
Embryonic tumors	−	−	−	−	−	−	−	0

+, present; −, not present; n, not reported; [a], died of pulmonary infection.